Design, Modeling and Control of a Novel Architecture for Automatic Transmission Systems

A THESIS
SUBMITTED TO THE FACULTY OF THE GRADUATE SCHOOL
OF THE UNIVERSITY OF MINNESOTA
BY

Virinchi Mallela

IN PARTIAL FULFILLMENT OF THE REQUIREMENTS
FOR THE DEGREE OF
Master of Science

Dr. Zongxuan Sun

June, 2013

Acknowledgements

I would like to sincerely thank my advisor, Prof. Zongxuan Sun, for allowing me to work on this exciting project for my Master's thesis. He has been a constant source of inspiration and has helped me improve my technical as well as presentation skills. His deeper insights and his encouragement to pursue new ideas added greatly to my learning experience. I would like to express my gratitude for his referral to intern with the R&D group of General Motors and to interview with another company when I was looking for a job.

I would also like to thank Dr. Rajesh Rajamani and Dr. Demoz Gebre-Egziabher for accepting my request to serve as my examining committee. I would like to extend my thanks to all the members of our lab group – Pradeep, Azrin, Chien Shin, Yongsoon, Ke, Chen, Yu, Mike, Meng, and Yaoying, who have made my stay more memorable. I would also like to acknowledge the help Chien Shin provided me in setting up the experiment.

I would like to thank the Transmission Lab Systems Group at General Motors, Dr. Kumar Hebbale, Dr. Dongxu Li for providing me with everything I needed to obtain the invaluable learning and experience and Dr. Chi-Kuan Kao for extending the internship opportunity to me.

Last but not the least, I would like to thank my parents and brother for constantly supporting me throughout my course of study. I would not be the person I am without their love and encouragement.

Dedication

To my family and friends

Abstract

Automotive transmissions are required to efficiently transfer energy from the engine to the wheels. Automatic transmissions are one of the most widely used transmission systems in the United States. This transmission houses a hydraulic system which is used to actuate the clutch system to realize different gear ratios. Currently, these clutches are primarily controlled in open-loop using hydraulic valves in a physical embodiment designed specifically for a given transmission system in order to perform precise pressure and flow control. To meet the increasing demand for higher fuel economy, transmissions with greater number of gear ratios are being introduced. The hydraulic architecture is becoming increasingly complicated with more clutches and control elements. With the advancement of MEMS technology, the sensor-based direct feedback control of clutches becomes possible. This paper first analyzes the current architecture of transmission hydraulic system and then presents a new architecture for the feedback-based clutches. The proposed architecture is further validated through experiments using hardware-in-the-loop system.

Contents

List of Tables

List of Figures

Chapter 1

Introduction

1.1 Background and Motivation

With increasing concerns about fuel economy, the demand to produce and transmit energy efficiently is more than ever. The internal combustion engine operates at widely varying efficiencies under different loading conditions. Automotive transmissions are thus used to operate the engine at more efficient operating points and also transfer the torque in a smooth manner. Many transmission systems have been developed over the years [1] to optimize the engine operating conditions by varying gear ratios between the input and output. Automatic transmissions (AT) are extensively used in North America. Other transmissions include manual transmission (MT) [2], automated manual transmission (AMT) [3, 4], dual-clutch transmission (DCT) [5, 6, 7], hybrid transmissions [8, 9, 10], and continuously variable transmission (CVT) [11, 12]. The challenges associated with each of the transmissions has been documented in [13]. MTs and AMTs have an inherent issue of torque interruption during gearshifts. DCTs may experience driveline vibrations during gearshifts, due to the absence of torque converters which provide damping. Hybrid transmissions require an additional power source and are expensive due to the complexity. CVTs provide the flexibility to run the engine at more efficient operating points due to the ability to vary the ratios. But mainly belt CVTs have been mass produced so far which have limited torque capacities. It is, therefore, still desirable to use stepped gear ATs in automotive applications.

The transmissions use clutches to accomplish the gear ratio variation. A clutch is a

mechanical device that transfers power between two rotating shafts. While one shaft is usually connected to an engine or a motor, the other shaft usually provides the output work. The clutch is a disc mounted on one shaft and is actuated to squeeze against the other shaft. Due to the friction between the components, torque starts getting transferred and slip speed between the shafts eventually reduces to zero or the desired value. Traditionally, it is actuated using hydraulics. There are two different types of clutches, dry [14] and wet [15]. A wet clutch is immersed in lubricating fluid that keeps the surface clean, and gives a smoother performance and longer life. Typically, multiple clutch plates are used to compensate for the smaller friction coefficients. But, some of the energy is lost to the fluid. Their motion is relatively small and restricted to a maximum of $1-3\,\text{mm}$. On the other hand, dry clutches, as the name suggests, are dry. It is not very uncommon to find a dry clutch with a single clutch plate as the friction is higher. The displacement of a dry clutch is higher to up to $7-10\,\text{mm}$, which makes it suitable for implementing a displacement sensor based control. The dry clutches are normally air-cooled.

Figure 1.1 shows the cross-section of an automatic transmission. ATs use a combination of electro-hydraulic wet clutches and planetary gear sets to achieve different gear ratios. Their arrangement for a 4-speed transmission [16] is shown in 1.2. The transmission architecture for a General Motors 4-speed transmission has been discussed in [17]. An in-house hydraulic system is used to actuate the clutches, which are controlled using control elements like Transmission Electro-Hydraulic Control Module (TEHCM) and valve body. Both the elements consist of different types of Variable Bleed Solenoid (VBS) valves. A two-stage control is achieved by these components to precisely control pressure and flow into the clutch chamber as there is no sensor feedback available in the existing system. The pilot pressure signals are generated by TEHCM and are used by the valve body to produce the required flow. The basic structure of the hydraulic architecture is similar in all the existing systems. Figure 1.3 summarizes the current architecture.

A hydraulic architecture for ATs is modeled and analyzed in [18, 19, 20]. Instead of the VBS valve, Pulse-Width Modulated (PWM) solenoid valve is used to generate the pressure signal. Based on this signal, a pressure control valve modulates the pressure of the line supplying fluid to the clutch. [21] used linear solenoid valves to generate

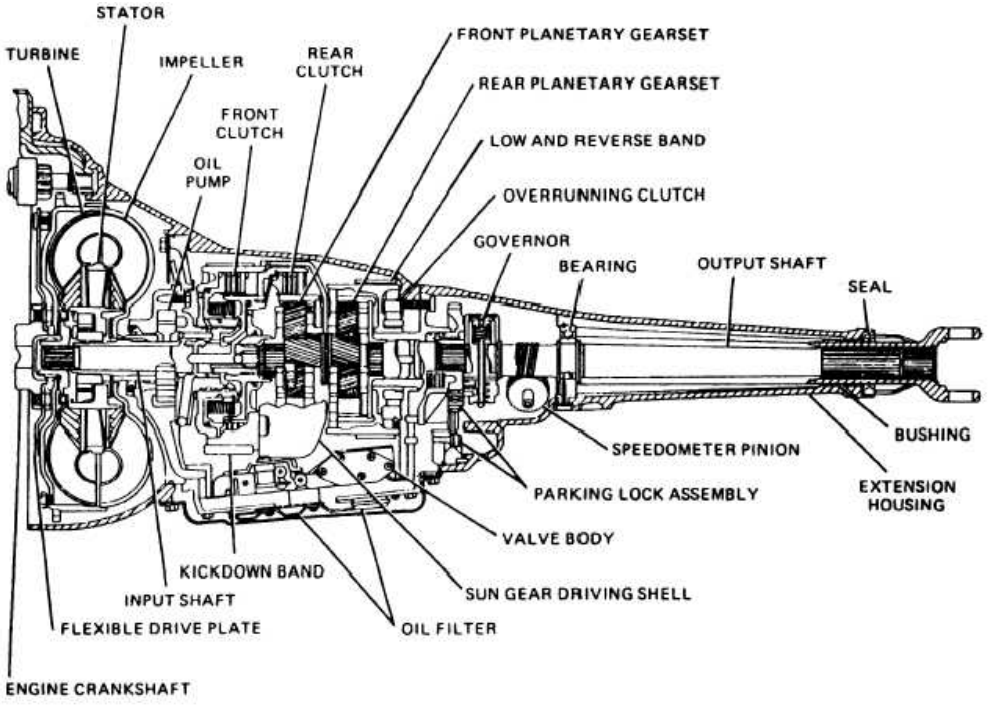

Figure 1.1: Cross-section of an Automatic Transmission

pressure signals which are sent to relay valves to control clutches. In [22], solenoid valves and directional valves are used to perform similar functions. The inlet pressure control for clutches performing gear shifts were separated by using additional shift and linear solenoid valves in Honda's 4-speed transmission [23]. The pressure control valves were later eliminated by redesigning the linear solenoid valves in [24]. The Toyota's 6-speed transmission in [25] uses large-flow small solenoids and manual shift valves to reduce the number of valves while increasing the calibration effort.

The number of speeds in stepped gear ATs has been increasing consistently [26] and is competing with CVTs in terms of achieving optimal performance for the engine. This is resulting in the increasing number of planetary gear sets being used in ATs. They require more clutches and other control elements, which adds to the complexity of the architecture. Certain logic valves in the valve body would have to be redesigned as they are specifically machined for a given transmission system. The flow requirements of

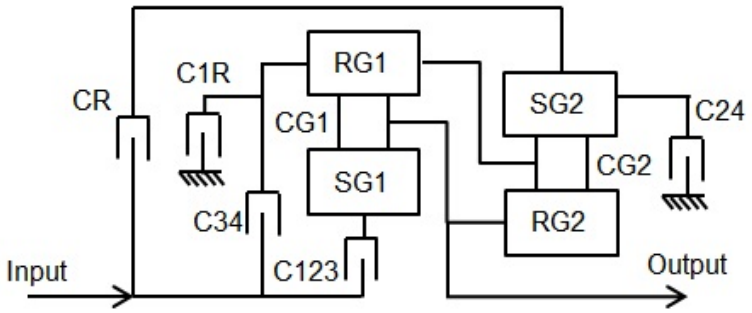

Figure 1.2: A 4-speed Automatic Transmission

the transmission are also increasing with the increase in the number of components due to the leakages [17]. During a gear shift, clutch-to-clutch shift control is performed by releasing one of the two engaged clutches and engaging another clutch in a synchronized way in order to continuously transmit torque to the wheels [27, 28, 29]. This shift control is performed almost entirely in open-loop due to spatial and cost constraints to embed a sensor into the clutch except for the limited feedback from speed sensors at the input and output of transmission thus requiring extensive calibration. It is, therefore, imperative to take a step back to analyze and redesign the overall architecture of the ATs in order to simplify the overall design and to improve the transmission efficiency.

In recent years, MEMS-based sensors have become more economically viable which makes them suitable for automotive control [30]. A pressure-based feedback control for an electro-hydraulic clutch was developed by [31]. Leveraging this idea, the proposed architecture is designed for similar clutches fitted with pressure sensors. The hydraulic control architecture could be simplified due to the addition of feedback. There are three main advantages of the new architecture. First, the new architecture provides flexibility to accommodate additional clutches into it without modifying any existing components. Second, due to the simplified design, fewer components are required. This would reduce the leakage losses in the system and in turn, the pump can be downsized. Finally, the quality of gear shifts can be improved as pressure feedback gives an accurate estimate of the torque capacity of a clutch.

The model for the new architecture has been built using MATLAB/SimHydraulics

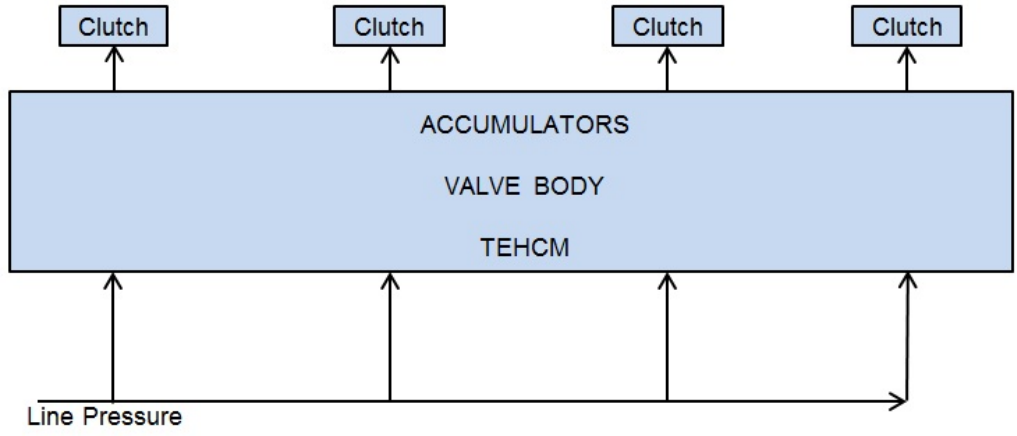

Figure 1.3: Current Architecture

along with the entire powertrain to analyze its performance. To further validate its performance, experiments have been conducted in a hardware-in-the-loop (HIL) environment. A HIL simulation using a real-time control module for AMTs was performed in [4] . A HIL platform was built using a commercial software (dSPACE), to study the AT characteristics by performing calculations in real-time [32, 33, 34, 35]. A pair of electric motors were controlled by multiprocessor computers to simulate the load experienced by transmission in [36]. A real hydraulic valve was operated in a HIL fashion as part of a complete powertrain model in [37]. In this thesis, the HIL simulation is executed using a real clutch setup while the entire driveline model is simulated. The real clutch is synchronized with the simulated clutches during gear shifts to analyze the performance of the architecture and the results thus obtained have been discussed.

1.2 Organization of the Thesis

The rest of the document is organized as follows:

Chapter 2 explains the layout and benefits of the proposed architecture over the existing architecture. It also discusses the models of all the components of the automotive powertrain gathered from the literature necessary to validate the new architecture.

Chapter 3 presents the control method employed to determine and perform clutch-to-clutch shift for this new architecture. The various levels of controllers are discussed. Also, the procedure and the mathematical basis for the implementation of different shifts are provided.

Chapter 4 introduces the hardware-in-the-loop simulation and describes the experimental setup. The clutch characteristics are identified experimentally. The experimental results pertaining to its operation over an entire EPA FTP cycle to test for reliability under different operating conditions are presented. Gear shifts representing the performance over the cycle are selected and discussed to demonstrate the shift quality.

Chapter 5 summarizes the research and proposes possible future extensions of the work.

Chapter 2

Proposed Architecture and Powertrain Modeling

2.1 Proposed Architecture

The electro-hydraulic clutches control the path of power flow through the planetary gear sets in the automatic transmissions. They are actuated by a hydraulic system housed inside the transmission. Traditionally, these clutches are controlled electronically using different stages of valves. A simple sketch of the current architecture is shown in Fig. 1.3. The Transmission Electro-Hydraulic Control Module (TEHCM), valve body and accumulators are used to control the fluid between pump and the clutches. They perform a two-stage control on pressure and flow rate of the fluid flowing into the clutches using Variable Bleed Solenoid (VBS) valves. TEHCM generates pressure signals which are then used by the valve body to produce the required flow. Due to the large number of components in this hydraulic system, the leakages in the system are significant[17] which require a larger pump. These components are necessary to precisely control the clutch with the existing architecture as there is no feedback available. During gearshifts, only feedback from speed sensors is used [27]. The clutch torque or its capacity cannot be detected directly since the current architecture does not employ any other sensors. Instead, a feedforward control is designed based on extensive calibration of the transmission under various operating conditions.

The proposed architecture for the hydraulic system of the automatic transmission

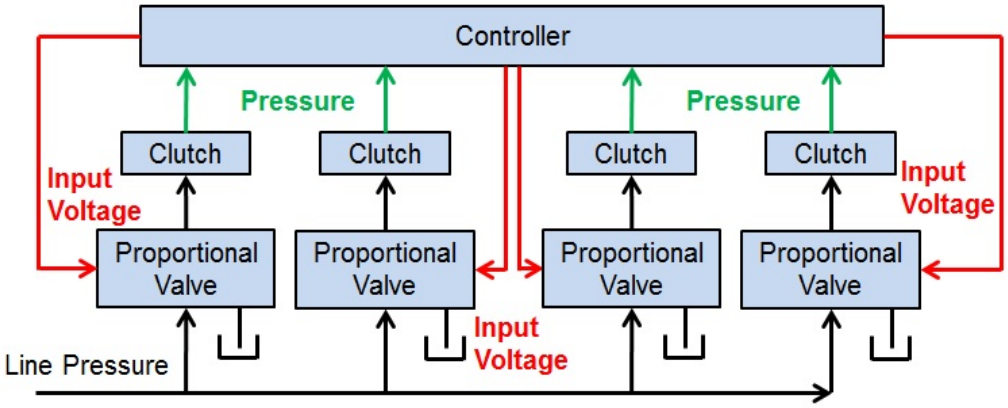

Figure 2.1: Proposed Architecture

system is shown in Fig. 2.1. The architecture has been very much simplified due to the addition of sensor feedback with the control distributed to individual clutch units. The clutch units are fitted with a pressure sensor inside the chamber and this feedback is used to control the clutches. Displacement sensors are difficult to implement due to spatial constraints. The VBS valves in TEHCM and valve body have been replaced by simple 2-position 3-way proportional pressure reducing valves.

It can be seen that while progressing from a transmission requiring n clutches to $n+1$ clutches, an additional clutch could be added easily to the architecture without requiring any modifications. The only other component required apart from the clutch is a proportional pressure reducing valve. To achieve the same in conventional architecture would be difficult since the control architecture would require redesign of the valve body to accommodate the additional clutch and its associated components. Furthermore, the number of components used for control are reduced which would reduce the leakage losses occurring in the system. As a result, the pump can be downsized as the flow requirement from the system goes down. During gear shifts, pressure sensor feedback from the clutch chamber can be used in addition to the speed sensors to improve shift quality, as it is related to the torque capacity of the clutch as explained in Sec. 2.2.5.

In order to evaluate the performance of this new architecture, an evaluation criteria has to be defined. Since the only way to gauge the performance of a transmission is by

implementing it in a powertrain, the complete model of an automotive drivetrain is built using various models from literature. Under steady gear conditions, this architecture is no different from the traditional architecture in terms of its output performance. The clutches are fully engaged and the torque carried by the clutches is typically lower than their capacities which allows it to transmit completely. Without a complete hydraulic setup, it is difficult to accurately predict the peak and average flow rate consumption. During gear shifts, the behavior of this new architecture can be studied by applying the same control methods used currently while utilizing the additional feedback element.

2.2 Powertrain Modeling

The schematic of an automotive powertrain is shown in Fig. 2.2. The engine is connected to the pump end of the torque converter which is a fluid coupling that dampens the vibrations in the driveline. The turbine end of the torque converter is connected to the transmission. The transmission encloses the planetary gear sets and the hydraulic system used for clutch actuation. The clutches are engaged to the planetary gears to realize different gear ratios between the transmission input and output. The output of the transmissions connects through the differential to the vehicle.

In order to test the proposed architecture, the hydraulic system has been simulated using SimHydraulics package of MATLAB/Simulink. The remaining components of the powertrain are coded as m-functions. The mathematical models for all the components used in the powertrain are provided in this section.

2.2.1 Engine

The engine is modeled as a torque source that can produce the desired torque. The loading on the engine is due to the torque converter, which connects it to the rest of the driveline. So, the engine speed depends on the entire driveline dynamics of the vehicle. The engine and torque converter models are provided in [38]. The engine dynamics can be described by:

$$J_e\dot{\omega}_e = T_e - T_p - T_f \tag{2.1}$$

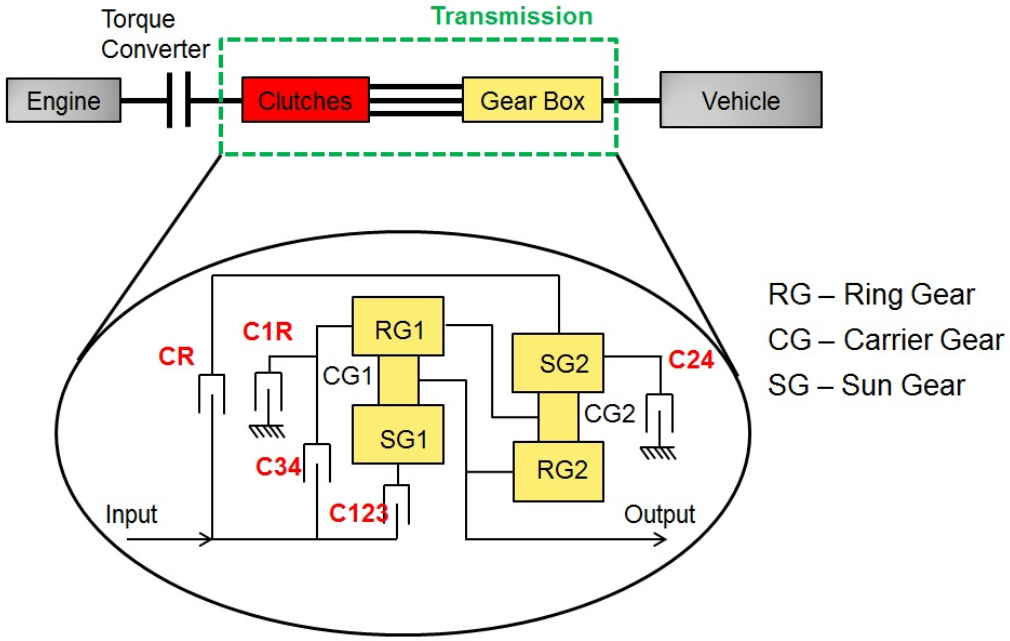

Figure 2.2: Automotive Powertrain with a blown-up view of transmission

where J_e is the inertia of the engine, ω_e is the engine speed, T_e is the torque generated by the engine and treated as the input, T_p is the pump torque of the torque converter, and T_f is the friction torque on the engine given by

$$T_f = 0.1056\,\omega_e + 15.10 \tag{2.2}$$

2.2.2 Torque Converter

The torque converter damps the driveline vibrations as it is a fluid coupling that connects the engine to the transmission and vehicle. It has three components: the impeller or pump, the stator, and the turbine. The pump side of the torque converter loads the engine and rotates at its speed. It pushes the fluid to the turbine side and rotates it. The turbine finally drives the load. The fluid is recirculated back to the impeller through the stator which guides it appropriately. The torque converter operates under two modes, converter and fluid-coupling. In the converter mode, the pump and turbine operate separately, while in the fluid coupling mode, the pump and turbine are locked

down and rotate together. The equations describing the two modes are given in [39]:

$$T_p = 3.4325 \times 10^{-3}\omega_p^2 + 2.2210 \times 10^{-3}\omega_p\omega_t - 4.6041 \times 10^{-3}\omega_t^2 \tag{2.3}$$

$$T_t = 5.7656 \times 10^{-3}\omega_p^2 + 0.3107 \times 10^{-3}\omega_p\omega_t - 5.4323 \times 10^{-3}\omega_t^2 \tag{2.4}$$

for converter mode (i.e., $\omega_t/\omega_p < 0.9$) and:

$$T_p = T_t = -6.7644 \times 10^{-3}\omega_p^2 + 32.0084 \times 10^{-3}\omega_p\omega_t - 25.2441 \times 10^{-3}\omega_t^2 \tag{2.5}$$

for fluid coupling mode (i.e., $\omega_t/\omega_p \geq 0.9$), where T_p and T_t are pump and turbine torques, and $\omega_p(=\omega_e)$ and ω_t are pump and turbine speeds. This model reaches engine idling condition at $70.49\,\text{rads}^-1$ or 673.1 RPM by setting $\omega_t = 0$ and idling torque of the engine at 18.16 Nm.

The transmission consists of two sets of planetary gear sets, electro-hydraulic clutches and an in-house hydraulic system to actuate the clutches.

2.2.3 Hydraulic Pump

A small internal-external crescent gear pump [17] model is used as the hydraulic pressure source. It consists of an inner gear and outer gear as shown in Fig. 2.3 (Source: [17]). It is a fixed displacement pump. If the inner gear completes one revolution, the volume of fluid transported between the inlet and discharge ports is equal to one-half of the volume enclosed between the addendum and dedendum circles of the gear. The displacement and flow rate of this pump are given by:

$$D_{\text{disp}} = \pi b_g[r_{a_1}^2 - (r_{a_2} - e_g)^2] \tag{2.6}$$

$$Q_t = D_{\text{disp}} N_p \tag{2.7}$$

where b_g is the gear width, r_{a_1} and r_{a_2} are the addendum radius of inner and outer gears, e_g is the distance between their centers, and N_p is the angular velocity of the pump.

The leakage in the pump due to the pressure difference between the ports is given by

$$Q_{lk} = \frac{10\pi d_{mg} c_r^3}{\mu(d_d - d_s)} \left[1 + 1.5\left(\frac{e_c}{c_r}\right)^3\right] \Delta P \tag{2.8}$$

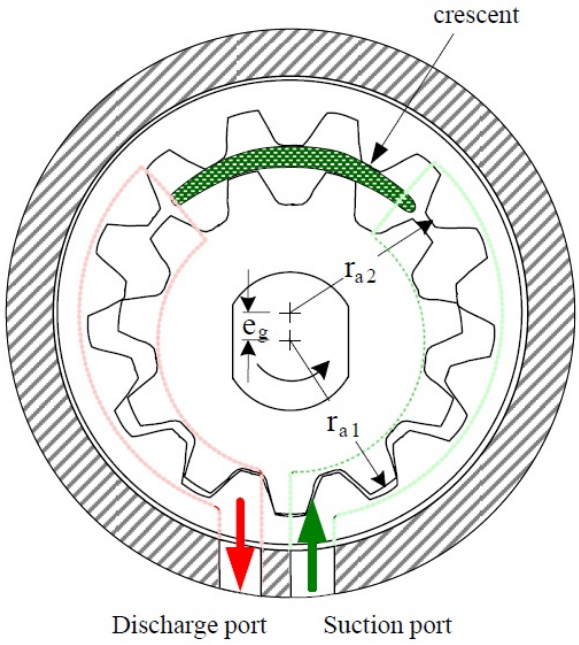

Figure 2.3: Internal-External (I-X) Crescent Gear pump

To account for the losses due to the rotational speed of the pump, the general expression for total leakage is written as

$$Q_{lk} = K_1 \Delta P + K_2 N_p \tag{2.9}$$

where K_2 is an experimentally determined coefficient.

2.2.4 Piping

The piping between the pump and the clutches has a fixed volume. The only dynamics in this part are that of pressure. The inflow is due to the pump and the outflow is into the clutches. Therefore, the pressure dynamics model for the piping can be written as:

$$\dot{P}_{\text{pipe}} = \frac{\beta(P_{\text{pipe}})}{V_{\text{pipe}}}(Q_t - Q_{lk} - Q_{C1R} - Q_{C123} - Q_{C34} - Q_{C24}) \tag{2.10}$$

where P_{pipe} is the pressure of the fluid in the pipe, V_{pipe} is the volume of the piping, and Q_{C1R}, Q_{C123}, Q_{C34}, and Q_{C24} are the flow rates into clutches C1R, C123, C34, and C24 respectively.

2.2.5 Clutch System

A standard clutch used in the current automotive systems has been used for the simulation and the subsequent experiments. The clutch chamber is fitted with a pressure sensor and its inlet is connected to a proportional valve as shown in Fig. 2.4. The proportional valve is a 3-way valve connecting the clutch chamber to the pump and tank respectively depending on the voltage applied. It has been modeled in [31].

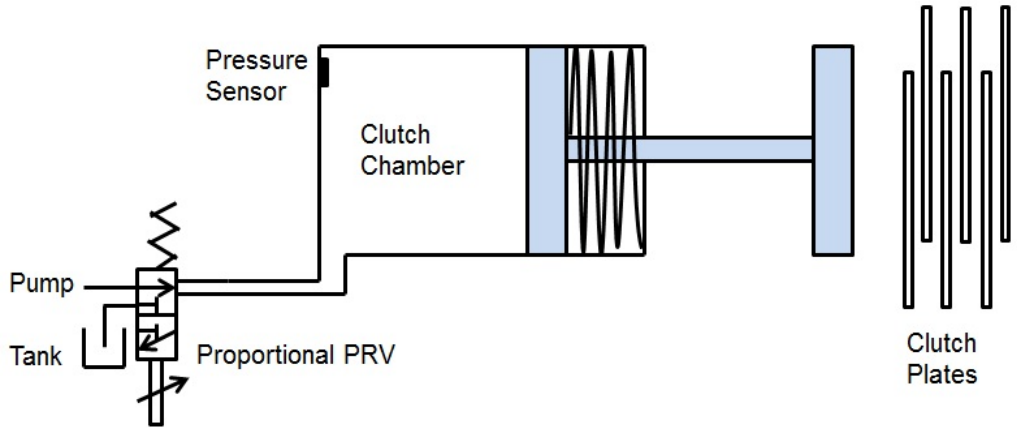

Figure 2.4: Clutch System

Proportional Pressure-Reducing Valve Dynamics

The proportional pressure reducing valve operates as a 3-way 2-position valve as shown in Fig. 2.5 (Source: [31]). It is used to control the clutch chamber pressure based on the input voltage. The input voltage controls the spool position of the valve ensuring the appropriate amount of orifice is open. When there is no control voltage, the spool is kept at the the top position by the return spring. The spool dynamics are described as follows:

$$\dot{L}_{\text{spool}} = v_{\text{spool}} \tag{2.11}$$

$$\dot{v}_{\text{spool}} = \frac{1}{M_{\text{spool}}}[F_{\text{mag}}(Vol) - K_{\text{spring}}(L_{\text{spool}} + L_{\text{preload}}) - D_{\text{spool}}v_{\text{spool}} - A_{\text{spool}}P_r] \tag{2.12}$$

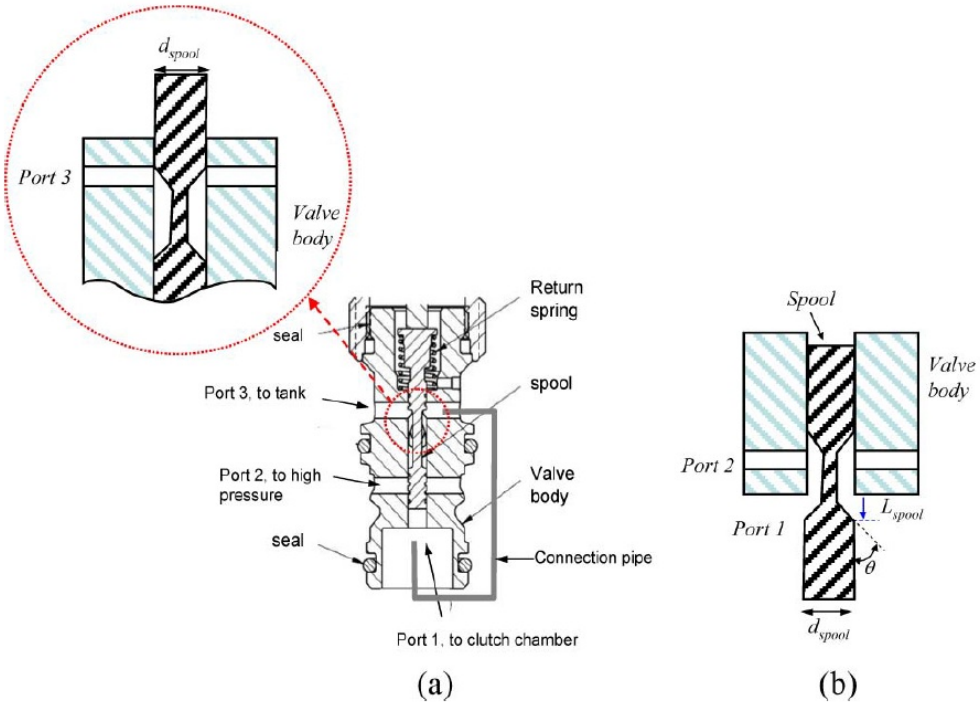

Figure 2.5: Cross-sectional view of the proportional pressure-reducing valve (a) Spool at tank port (b) Spool at the clutch chamber port

where L_{spool} is the spool position, v_{spool} is the spool velocity, M_{spool} is the spool mass, K_{spring} is the spool spring constant, L_{preload} is the spring preload, A_{spool} is the cross-sectional area of the spool, D_{spool} is the damping coefficient, and P_r is the clutch chamber pressure (gauge). $F_{\text{mag}}(Vol)$ is the force applied by the solenoid on the spool given by:

$$F_{\text{mag}}(Vol) \;=\; K_f \times i = K_f \times \left(\frac{i_{\max} - i_{\min}}{Vol_{\max}} \, Vol + i_{\min} \right) \tag{2.13}$$

where K_f is the coil magnetic constant, $i_{\max}$ and $i_{\min}$ are the maximum and minimum currents that can be generated from the power amplifier, and $Vol_{\max}$ is the maximum control voltage corresponding to $i_{\max}$. The area between the high pressure port and the clutch chamber port is dependent on the spool position L_{spool} as follows:

$$A_{\text{orifice}}(L_{\text{spool}}) \;=\; \pi L_{\text{spool}} \sin(\theta) \times (d_{\text{spool}} - L_{\text{spool}} \sin(\theta) \cos(\theta)) \tag{2.14}$$

where d_{spool} is the diameter of the spool, and θ is the spool surface slant angle. Similarly, the orifice area A_{dump} between the clutch chamber port and the tank port is given by

$$A_{\text{dump}}(L_{\text{spool}}) \;=\; -\pi L_{\text{spool}} \sin(\theta) \times (d_{\text{spool}} + L_{\text{spool}} \sin(\theta) \cos(\theta)) \tag{2.15}$$

The flow dynamics across the valve orifice is given by

$$Q(L_{\text{spool}}, P_r) \;=\; \begin{cases} A_{\text{orifice}}(L_{\text{spool}})\, C_d \sqrt{\dfrac{2|P_h - P_r|}{\rho}}\, \text{sign}(P_h - P_r), & (L_{\text{spool}} > 0) \\ 0, & (L_{\text{spool}} = 0) \\ A_{\text{dump}}(L_{\text{spool}})\, C_d \sqrt{\dfrac{2|P_r|}{\rho}}, & (L_{\text{spool}} < 0) \end{cases} \tag{2.16}$$

Clutch Piston Dynamics

The dynamics of clutch motion are described by the following state equations:

$$\dot{x}_1 \;=\; x_2 \tag{2.17}$$

$$\begin{aligned} \dot{x}_2 \;=\; & \frac{1}{M_p} \times [A_p \times (P_r + P_c) - K_p(x_1 + x_{p0}) - D_p x_2 \\ & - F_{\text{drag}}(P_r + P_c) - F_{\text{eng}}] \end{aligned} \tag{2.18}$$

where x_1 is the clutch piston displacement, x_2 is the clutch piston velocity, M_p is the effective mass of the piston, A_p is the piston surface area, K_p is the clutch spring stiffness, x_{p0} is the return spring preload, D_p is the clutch damping coefficient, and P_c is the centrifugal force induced pressure generated from the rotation of the clutch assembly. F_{drag} is the piston seal drag force, which is dependent on the piston motion. It is modeled as

$$F_{\text{drag}} \;=\; \begin{cases} \{[k_m(P_r + P_c) + c_m] \times \text{sign}(x_2), & (x_2 \neq 0) \\ F_{\text{stick}}, & (x_2 = 0) \end{cases} \tag{2.19}$$

where F_{eng} is the force exerted by the clutch plates on the clutch piston after fill and during engagement. F_{stick} is the static friction on the piston which can be written as:

$$F_{\text{stick}} \;=\; \begin{cases} \{[k_s(P_r + P_c) + c_s] \times \text{sign}(F_{\text{net}}), & (|F_{\text{net}}| \geq |F_{stick}|) \\ F_{\text{net}}, & (|F_{\text{net}}| < |F_{stick}|) \end{cases} \tag{2.20}$$

where F_{net} is the net driving force on the piston.

Pressure Dynamics

Pressure dynamics need to be considered whenever the fluid either enters or exits the clutch chamber. It is described by the following equation:

$$\dot{P}_r = \frac{\beta(P_r)}{V}(Q(L_{\text{spool}}, P_r) - A_p\dot{x}_2) \tag{2.21}$$

where V is the chamber volume, which is assumed constant due to small clutch piston displacement, and β is the effective bulk modulus. The entrained air in oil could cause the variation of bulk modulus with the pressure in the clutch chamber, especially during clutch fill when the pressures are low. The bulk modulus model used in the simulations is obtained from SimHydraulics as shown in Eq. (2.22).

$$\beta(P_r) = \beta_0 \frac{1 + R\left(\frac{P_a}{P_a + P_r}\right)^{\frac{1}{\gamma}}}{1 + R\frac{P_a^{\frac{1}{\gamma}}}{\gamma(P_a + P_r)^{\frac{\gamma+1}{\gamma}}}\beta_0} \tag{2.22}$$

where β_0 is the bulk modulus of the fluid with no air entrainment, γ is the ratio of specific heats for air, P_a is the atmospheric pressure, and R is the percentage of air entrained in the fluid by volume.

Reduced Order System

As described in [31], the dynamic response of the proportional valve is much faster as compared to the clutch dynamics. This would simplify the control design as the proportional valve spool dynamics are converted to static mapping.

$$L_{\text{spool}} = \frac{1}{K_{\text{spring}}}[F_{\text{mag}}(u) - K_{\text{spring}} \times L_{\text{preload}} - A_{\text{spool}}P_r] \tag{2.23}$$

where $u = Vol$ is the control input to the proportional valve. Therefore, the pressure dynamics will be modified to

$$\dot{P}_r = \frac{\beta(P_r)}{V}(Q(u, P_r) - A_p\dot{x}_2) \tag{2.24}$$

Finally, the reduced order system of the spool consists of equations 2.17, 2.18, 2.23 and, 2.24.

Clutch Torque

The clutch transmits torque by squeezing the clutch plates together. The torque capacity of the clutch depends on the force applied by the clutch piston on the plates and is also the maximum torque that a clutch can transmit which is given by:

$$T = \mu(\omega_{\text{slip}}) n R_{\text{mean}} F_{\text{eng}} \tag{2.25}$$

where R_{mean} is the mean radius of the clutch, and n is the number of clutch packs. $\mu(\omega_{\text{slip}})$ is the coefficient of friction dependent on the slip speed between the clutch plates as shown in 2.6. Normally, it is expected that the static friction coefficient is greater than the kinetic friction coefficient. But it induces the problem of clutch judder which has been discussed in [40]. This problem has already been tackled in the previous decade and clutches with greater kinetic friction coefficient have been designed by various manufacturers [40, 41].

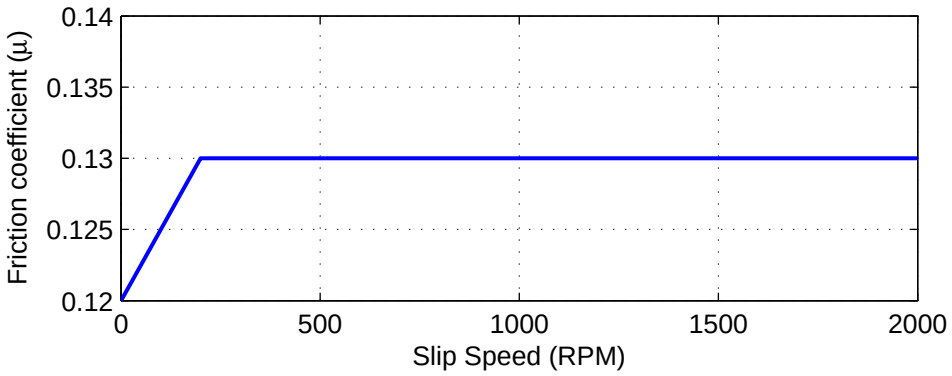

Figure 2.6: Variation of friction coefficient with slip speed

The curve used for determining the engagement force, F_{eng}, in the simulated clutches C1R, C123, and C34 is shown in 2.7.

The engagement force for clutch C24 is estimated using pressure-displacement data from the experiments and is discussed further in Section 4.2. All the clutches are assumed to modeled in the same way but with different dimensions in order to account for the difference in their torque capacities.

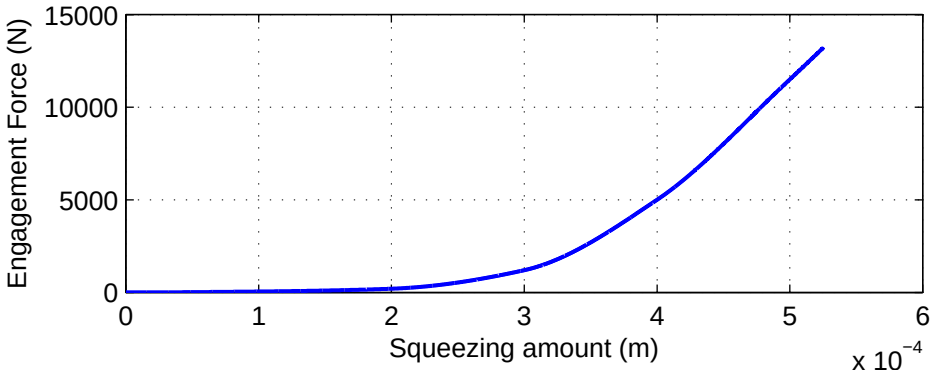

Figure 2.7: Engagement Force vs Clutch Displacement after fill for C1R, C123, and C34

2.2.6 Gearbox

The planetary gear sets enable the transmission to achieve desired ratios by engaging a defined set of clutches. To monitor the quality of the shift, it is important to understand and model the dynamics of these planetary gear sets. For a 4-speed transmission, the ring gear of the first planetary gear set is rigidly connected to the carrier of the second, and the ring gear of the second planetary gear set is rigidly connected to the carrier of the first as shown in Fig 2.8. The effect of backlash within the gear sets has not been considered for this analysis.

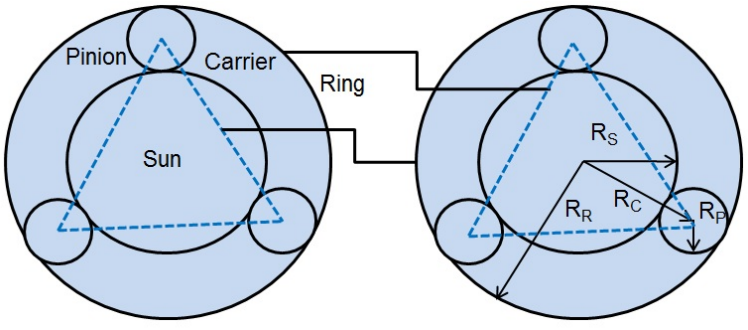

Figure 2.8: Planetary gear sets in a 4-speed transmission

Given these constraints and the location of the clutches, the motion of the all the

gears can be predicted by calculating the motion of any two gears. The complete derivation for these gear sets has been performed using Lagrangian formulation in [42]. It is possible to implement a continuous model during gear shifts using this model. By defining the angles of rotation of the sun, carrier, pinion, and ring gears as α, β, γ and θ, we can write the dynamics of a 4-speed transmission as:

$$\begin{bmatrix} B_{11} & B_{12} \\ B_{21} & B_{22} \end{bmatrix} \begin{bmatrix} \ddot{\theta}_1 \\ \ddot{\theta}_2 \end{bmatrix} = \begin{bmatrix} -A_2 & 0 & A_4 & 1 \\ A_1 & 1 & -A_5 & 0 \end{bmatrix} \begin{bmatrix} T_{S_1} \\ T_{C_1R_2} \\ T_{S_2} \\ T_{C_2R_1} \end{bmatrix} \tag{2.26}$$

where T_{S_1}, $T_{C_1R_2}$, T_{S_2}, and $T_{C_2R_1}$ are torque inputs at the sun and ring gears of the first and second planetary gears respectively. The radius of the sun(R_S), pinion(R_P) and the ring gear(R_R) are constrained by the equation, $R_R = R_S + 2R_P$.

The elements of the coefficient matrix can be calculated by using the following:

$$A_1 = 1 + A_2 \ , \qquad A_2 = \frac{R_{R_1}}{R_{S_1}} \ , \qquad A_3 = \frac{R_{R_1}}{R_{P_1}}$$

$$A_4 = 1 + A_5 \ , \qquad A_5 = \frac{R_{R_2}}{R_{S_2}} \ , \qquad A_3 = \frac{R_{R_2}}{R_{P_2}}$$

$$\begin{aligned} B_{11} &= A_2^2 I_{S_1} + n_1 A_3^2 I_{P_1} + I_{C_2R_1} + A_4^2 I_{S_2}^2 + n_2[A_6^2 I_{P_2} + m_{P_2}(R_{S_2} + R_{P_2})^2] \\ B_{12} &= B_{21} = -A_1 A_2 I_{S_1} - n_1 A_3^2 I_{P_1} - A_4 A_5 I_{S_2} - n_2 A_6^2 I_{P_2} \\ B_{22} &= A_1^2 I_{S_1} + n_2 A_6^2 I_{P_2} + I_{C_1R_2} + A_5^2 I_{S_2}^2 + n_1[A_3^2 I_{P_1} + m_{P_1}(R_{S_1} + R_{P_1})^2] \end{aligned}$$

where I_{S_1}, I_{P_1}, $I_{C_1R_2}$, m_{P_1}, I_{S_2}, I_{P_2}, $I_{C_2R_1}$ and m_{P_2} are the moments of inertias of the sun, pinion, combined inertia of the carrier and the ring gear, and mass of the pinion gear of the first and second planetary gears respectively.

The accelerations of the remaining gears can be calculated from the ring gear accelerations, $\ddot{\theta}_1$ and $\ddot{\theta}_2$ by

$$\begin{bmatrix} \ddot{\alpha}_1 \\ \ddot{\gamma}_1 \\ \ddot{\alpha}_2 \\ \ddot{\gamma}_2 \end{bmatrix} = \mathbf{C} \begin{bmatrix} \ddot{\theta}_1 \\ \ddot{\theta}_2 \end{bmatrix} \tag{2.27}$$

where

$$\mathbf{C} = \begin{bmatrix} -A_2 & A_1 \\ A_3 & -A_3 \\ A_4 & -A_5 \\ -A_6 & A_6 \end{bmatrix} \tag{2.28}$$

The gear ratios used in this analysis are [2.393 1.450 1.000 0.670].

2.3 Vehicle Model

The transmission is followed by a differential which connects it to the wheels. The differential is modeled as a constant reducing gear pair with a ratio of r_{diff}. The vehicle experiences three types of resistances, namely, rolling, wind and grade resistances. The loads on a vehicle have been analyzed by [43], [44], and [45]. The rolling resistance is the friction force between the tire and the road surface given by:

$$RR = K_r M_v g \cos(\theta_g) \tag{2.29}$$

where K_r is the dimensionless rolling resistance coefficient, M_v is the mass of the vehicle, g is the acceleration due to gravity, and θ_g is the grade angle.

The wind resistance, as the name suggests, is the aerodynamic drag experienced by the vehicle is written as

$$WR = \frac{1}{2}\rho_a C_f A_f v^2 \tag{2.30}$$

where ρ_a is the density of air, C_d is the aerodynamic drag coefficient, A_f is the frontal area of the vehicle, and v is the vehicle speed.

The grade resistance is due to the gravity on roads with a gradient. Using the grade of the road, θ_g, the grade resistance can be computed by

$$GR = M_v g \sin(\theta_g) \tag{2.31}$$

So, the total resistive forces can be combined and written as

$$F_R = RR + WR + GR + F_{\text{braking}} \tag{2.32}$$

where F_{braking} is the load due to braking from the driver. It is input to the model as a map.

The vehicle inertia is reflected to the other side of the differential and lumped with the output gears of the planetary gear sets in this analysis. The entire load on the vehicle, therefore, is used as an input to the transmission. The total resistive torque due to vehicle acting on the transmission is

$$T_{C_1R_2} = -T_R = -F_r\, r_r \tag{2.33}$$

where r_r is the radius of the tire.

The parameters related to the simulation are tabulated in Tab. 2.1.

Table 2.1: Values of Parameters

Symbol	**Name**	**Value**
J_e	Engine Inertia	$0.1454\,\text{Kgm}^2$
J_t	Turbine Inertia	$0.05623\,\text{Kgm}^2$
b_g	Gear Width	$0.010013\,\text{m}$
r_{a_1}	Addendum radius of inner drive gear	$0.035131\,\text{m}$
r_{a_2}	Addendum radius of outer internal gear	$0.034245\,\text{m}$
e_g	Center distance	$0.007445\,\text{mm}$
N_p	Pump speed	$1500\,\text{RPM}$
c_r	Radial clearance	$0.002\,\text{m}$
μ	Absolute viscosity	$1.3603\,\text{cP}$
d_d	Dedendum diameter	$0.05\,\text{m}$
d_s	Shaft diameter	$0.01\,\text{m}$
e_c	Eccentricity	$0.003\,\text{m}$
V_{pipe}	Volume of piping	$1.7\text{e-}3\,\text{m}^3$
K_{spring}	Valve Spring stiffness	$1087.6\,\text{N/m}$
L_{preload}	Valve Spring Preload	$0.0067\,\text{m}$
A_{spool}	Valve Spool Cross-sectional area	$5.0645\text{e-}6\,\text{m}^2$
K_f	Coil magnetic constant	$22.7\,\text{N/A}$

Continued next page

Table 2.1 : Values of Parameters (contd.)

Symbol	**Name**	**Value**
$i_{\max}$	Maximum current from power amplifier	1.28 A
$i_{\min}$	Minimum current from power amplifier	0.25 A
$Vol_{\max}$	Maximum voltage	10 V
θ	Spool angle	$\pi/6$ rad
C_d	Coefficient of discharge	0.7
M_p	Clutch piston Mass	0.4 Kg
A_p	Clutch piston cross-sectional area	0.00628 m^2
K_p	Clutch spring stiffness	242640 N/m
x_{p0}	Clutch spring preload	0.0015928 m
D_p	Clutch piston damping	135.4 Ns/m
k_m	Kinetic friction coefficient	0.001517
c_m	Kinetic friction constant	5.22
k_s	Static friction coefficient	0.00153
c_s	Static friction constant	5.26
β_0	Bulk Modulus of oil	17000 bar
ρ	Oil density	880 Kg/m^3
R	Entrained air content	6%
γ	Ratio of specific heats	1.4
n_{C1R}	Number of clutch plates in C1R	7
n_{C123}	Number of clutch plates in C123	7
n_{C34}	Number of clutch plates in C34	5
n_{C24}	Number of clutch plates in C24	10
R_{C1R}	Mean radius of clutch C1R	0.0648 m
R_{C123}	Mean radius of clutch C123	0.0466 m
R_{C34}	Mean radius of clutch C34	0.0652 m
R_{C24}	Mean radius of clutch C24	0.0321 m
S_1	Number of Sun gear teeth - 1	56
R_1	Number of ring gear teeth - 1	78
P_1	Number of pinion gear teeth - 1	11

Continued next page

Table 2.1 : Values of Parameters (contd.)

Symbol	**Name**	**Value**
S_2	Number of sun gear teeth - 2	42
R_2	Number of ring gear teeth - 2	88
P_2	Number of pinion gear teeth - 2	23
R_{S_1}	Radius of sun gear - 1	0.046786 m
R_{R_1}	Radius of ring gear - 1	0.065166 m
R_{P_1}	Radius of pinions gears - 1	0.00919 m
R_{S_2}	Radius of sun gear - 2	0.031962 m
R_{R_2}	Radius of ring gear - 2	0.0669795 m
R_{P_2}	Radius of pinions - 2	0.017509 m
I_{S_1}	Moment of inertia of sun gear - 1	0.00102 $\mathrm{Kgm^2}$
$I_{C_1R_2}$	Moment of inertia of ring gear - 2 & carrier gear - 1	0.00902 $\mathrm{Kgm^2}$
I_{P_1}	Moment of inertia of pinion gear - 1	6.7295e-6 $\mathrm{Kgm^2}$
I_{S_2}	Moment of inertia of sun gear - 2	0.00452 $\mathrm{Kgm^2}$
$I_{C_2R_1}$	Moment of inertia of ring gear - 1 & carrier gear - 2	0.005806 $\mathrm{Kgm^2}$
I_{P_2}	Moment of inertia of pinion gear - 2	4.7637e-6 $\mathrm{Kgm^2}$
m_{P_1}	Mass of pinions gears - 1	0.060967 Kg
m_{P_2}	Mass of pinions gears - 2	0.053199 Kg
n_1	Number of pinions - 1	4
n_2	Number of pinions - 2	4
r_{diff}	Differential ratio	3.37
g	Acceleration due to gravity	9.8 $\mathrm{m/s^2}$
K_r	Rolling friction coefficient	0.015
M_v	Mass of the vehicle	1500 Kg
θ_g	Grade angle of road	0
ρ_a	Density of air	1.225 $\mathrm{Kg/m^3}$
C_f	Aerodynamic drag coefficient	0.3
A_f	Vehicle frontal area	2.35 $\mathrm{m^2}$
r_r	Radius of tires	0.325 m

Chapter 3

Control Methodology

The transmission is a very crucial component of a driveline since it affects the drivability and fuel efficiency. The control elements in the driveline are the electro-hydraulic clutches. As mentioned in previous chapter, the gear ratios are achieved by the planetary gear sets through the actuation of the electro-hydraulic clutches. Each ratio is referred to as a gear state and two clutches are engaged while in a gear state. A gear shift is performed through a clutch-to-clutch shift to continuously transmit torque without interruption. In a clutch-to-clutch shift, one of the two clutches disengages while a different clutch engages. The on-coming clutch is prepared to engage by moving it till it starts touching the clutch plates. This process is called clutch fill [13]. After the completion of clutch fill, the torques in the on-coming and off-going clutches are synchronized and the relation between them can be derived using lever diagram analysis [46]. In the current architecture, transmission control is performed in open loop or by using feedback from speed sensors [27, 28]. For the proposed architecture, the control is performed by two controllers using feedback from pressure sensor in addition to the speed sensors.

3.1 High-level Controller

The high-level controller determines the occurrence of the gear shift by using a shift scheduling chart. It is a lookup table that determines the gear shift based on the throttle input by the driver and the velocity of the vehicle as shown in Fig. 3.1. The

hysteresis between up-shift and down-shift ensures that there is no chattering during gear shifts.

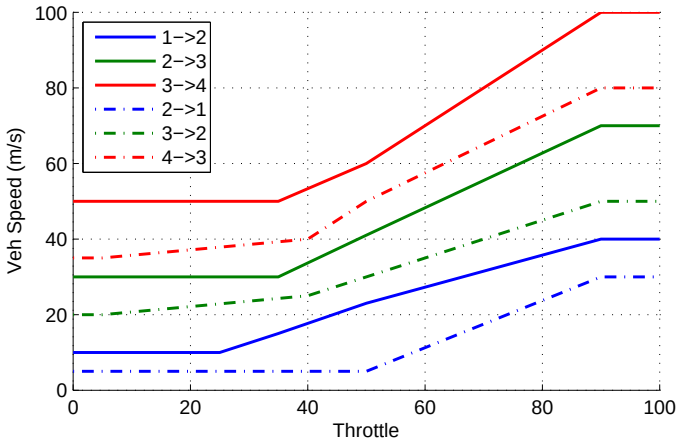

Figure 3.1: Shift scheduling graph showing up-shift and down-shift

3.2 Low-level Controller

To actually perform the shift, there is a lower level controller that synchronizes the on-coming and off-going clutches in a clutch-to-clutch shift. It uses the feedback from three sensors: Clutch chamber pressure sensor, Transmission Input Speed Sensor (TISS) and Transmission Output Speed Sensor (TOSS). It controls the clutches and their torque capacities by tracking trajectories which are either predetermined or generated in real-time during the shift. To perform pressure tracking, a PID controller has been used as shown in Eq. (3.1).

$$V = K_p\, e + \int K_i\, e\, dt + K_d\, \frac{de}{dt} \tag{3.1}$$

where V is the control input to the proportional pressure reducing valve, e is the error in pressure tracking, and K_p, K_i and K_d are calibrated constants of the PID controller.

To determine these reference pressure trajectories, it is required to understand the relation between torques carried by various clutches for each steady gear state and gear shift.

3.2.1 Steady Gear State

In order to design or control the clutches, the mechanism behind realizing the gear ratios in a transmission and the correlation between the torques transmitted has to be understood. Lever diagram is a useful tool to understand the gear ratio mechanics (Refer [46]). The lever diagram of a 4-speed automatic transmission system is shown in Fig. 3.2. This transmission consists of five clutches which are used in multiple combinations to achieve different gear ratios between the input and the output of the transmission. Three clutches (C123, C34 and CR) can directly connect the respective gears to the engine while two other clutches (C1R and C24) are used to ground the gears by locking them to the transmission casing. A planetary gear set is a two degree of freedom (2-DOF) system. Two of them are connected so that the combined DOF remains two. So, in the transmission system shown, only two of the five clutches are engaged at a time for each gear state. The clutch engagement schedule for this transmission is shown in Tab. 3.1. Since the clutch CR is used only for reverse gear, it has been ignored in the implementation.

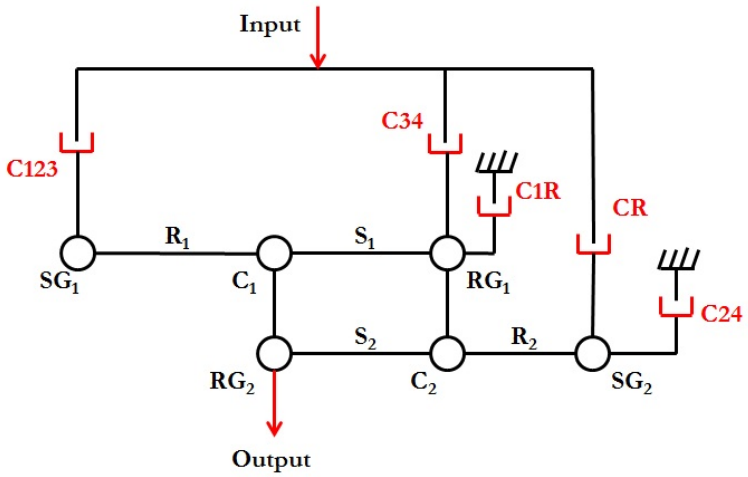

Figure 3.2: Lever diagram of 4-speed automatic transmission system

Each of the clutches carry different amount of torque depending on the gear state and the location where it is applied. The net torque from all the engaged clutches will

Table 3.1: Clutch Engagement Schedule

Gear	C1R	C123	C24	C34	CR
1	X	X	-	-	-
2	-	X	X	-	-
3	-	X	-	X	-
4	-	-	X	X	-
R	X	-	-	-	X

contribute towards the output. In the following sections, torques transmitted through different clutches while in gear and during shift are calculated.

When the vehicle is moving steadily in a given gear state, the torque from the engine is transferred to the vehicle through planetary gear sets. The clutches determine the path of power transfer and the ratio that is realized in that gear state. The equivalent lever diagram for the transmission in first gear is shown in Fig. 3.3. The input torque coming from the engine and through the torque converter is transmitted through clutch C123 only. The ring gear of the first planetary gear set is grounded using clutch C1R. By constraining two of the gears, the output torque of the transmission and the effective gear ratio can be calculated. The equations for this arrangement can be written as shown in Eq. (3.3) to Eq. (3.5).

$$T_{C123} = T_{in} \tag{3.2}$$

$$T_{C123}(R_1 + S_1) = T_{out}S_1 \tag{3.3}$$

$$T_{in}R_1 = T_{C1R}S_1 \tag{3.4}$$

$$=> T_{out} = (\frac{R_1 + S_1}{S_1})T_{in} \tag{3.5}$$

Similarly, the torque ratios with respect to the input torque in each of the clutches for various gears is shown in Table 3.2.

The automatic transmissions are designed such in a way that whenever a gear shift occurs, only one of the two clutches will be disengaged and a different clutch will be

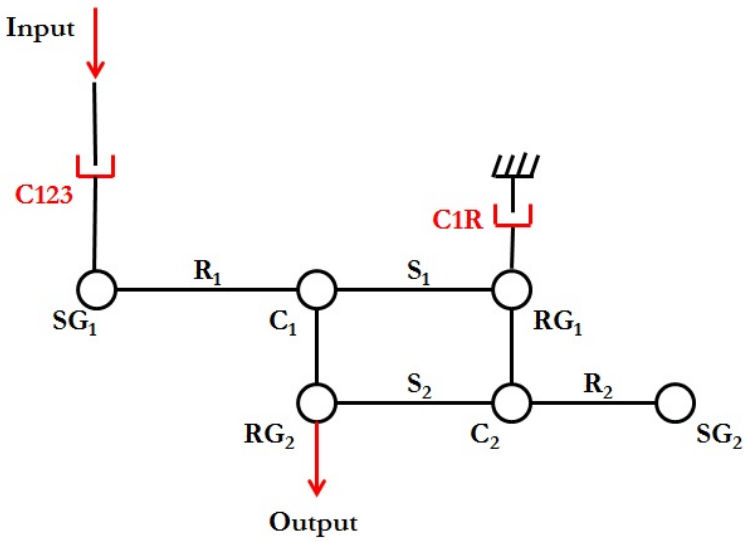

Figure 3.3: Lever diagram for 1^{st} gear

engaged. This is called single transition shift. It simplifies the control required for shift control. The on-coming and off-going clutches are to be synchronized based on the understanding of gear shifting mechanics in order to achieve a smooth gear shift.

3.2.2 Clutch Fill

Clutch fill is a crucial part for effective gear shift control [13]. Immediately after the value of the gear command changes, the clutch fill process begins for the on-coming clutch. This clutch is moved to a position where it is starts to touch the clutch plates, without squeezing them. It is then ready to be engaged. Additional motion can cause over-fill which will cause the clutch to start transmitting torque before it is desired. This can cause a partial tie-down of the transmission and will result in deceleration of the engine and the vehicle. Under-fill occurs when the clutch stops short of the desired fill position. In this case, it is difficult to synchronize the shift as the clutch is not ready to transmit torque and might lead to engine flare.

Since the clutch uses pressure feedback in this architecture, a pressure profile has been designed that ensures that the clutch piston overcomes the friction and spring force

Table 3.2: Torques in individual clutches ($\times T_{in}$)

Gear	C1R	C123	C24	C34	CR
1	$\frac{R_1}{S_1}$	1	-	-	-
2	-	1	$\frac{R_1 S_2}{S_1(R_2+S_2)}$	-	
3	-	$\frac{S_1}{R_1+S_1}$	-	$\frac{R_1}{R_1+S_1}$	-
4	-	$\frac{S_2}{R_2+S_2}$	-	1	
R	$1+\frac{R_2}{S_2}$	-	-	-	1

to achieve a good fill. The exact details will be discussed later in Sec. 4.2. Following the clutch fill, either up-shift or down-shift will be done depending on the gear command from the high-level controller.

3.2.3 Up-shift

Up-shift is defined as the gear shift occurring when the gear changes from a lower gear to a higher gear. The ratio between the input and output decreases after the shift. It has been illustrated using the example of a 1-2 up-shift. To accomplish this shift, clutch C1R needs to be released and clutch C24 needs to be applied while clutch C123 is kept engaged throughout the shift. Fig. 3.4 shows the lever diagram for the up-shift from 1^{st} to 2^{nd} gear. The on-coming clutch (C24) is filled while keeping the off-coming clutch (C1R) as it is. The relationship between the torque capacity of the clutch and the pressure in the clutch chamber has been discussed earlier in Sec. 2.2.5. Then, the pressure in the clutch C1R is reduced to a level where its torque capacity matches with the actual torque carried by the clutch. This is detected through a change in sign of the first derivative of the ratio between transmission input and output speeds. Immediately, the torque phase occurs when the torque from the clutch C1R gets completely transferred to the clutch C24 in a synchronized way based on Eq. (3.6) and Eq. (3.7)

. In order to avoid dealing with multiple-input multiple-output (MIMO) systems, the problem has been split into two independent single-input single-output (SISO) systems. The clutches, C1R and C24, are made to track two different pressure trajectories which would ensure that the clutches remain synchronized throughout the shift when tracked successfully (see Fig. 3.5).

$$T_{C1R} = T_{in}\frac{R_1}{S_1} - T_{C24}\left(\frac{R_2}{S_2} + 1\right) \tag{3.6}$$

$$T_{out} = T_{in}\left(\frac{R_1 + S_1}{S_1}\right) - T_{C24}\frac{R_2}{S_2} \tag{3.7}$$

where T_{in} is the input torque, T_{C1R} is the torque in clutch C1R, T_{C24} is the torque in clutch C24, and R_1, R_2, S_1, and S_2 are the number of teeth on ring gear and sun gear of the planetary gears.

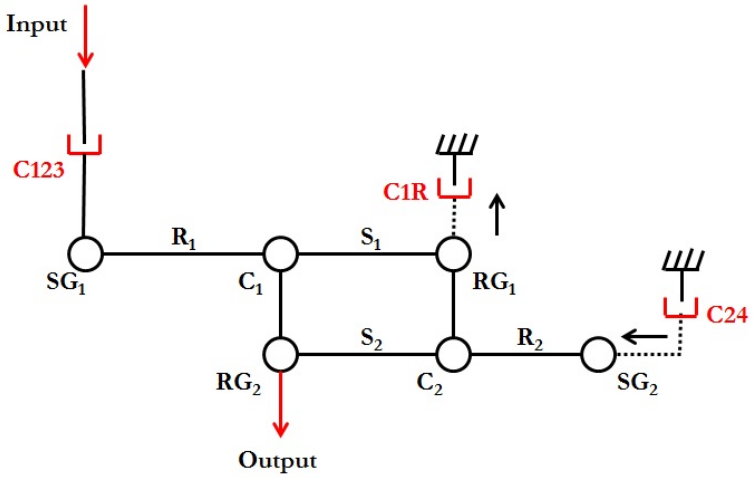

Figure 3.4: Up-shift from 1^{st} to 2^{nd} gear

It is then followed by the inertia phase (Eq. (3.8)) where the engine speed is brought to the desired value. After the clutch C1R completely disengages, the torque capacity of clutch C24 is further increased to its maximum to bring the system to the final ratio, thus completing the shift.

$$T_{out} = (T_{in} - I_{in}\alpha)\left(1 + \frac{R_1}{S_1}\frac{S_2}{R_2 + S_2}\right) \tag{3.8}$$

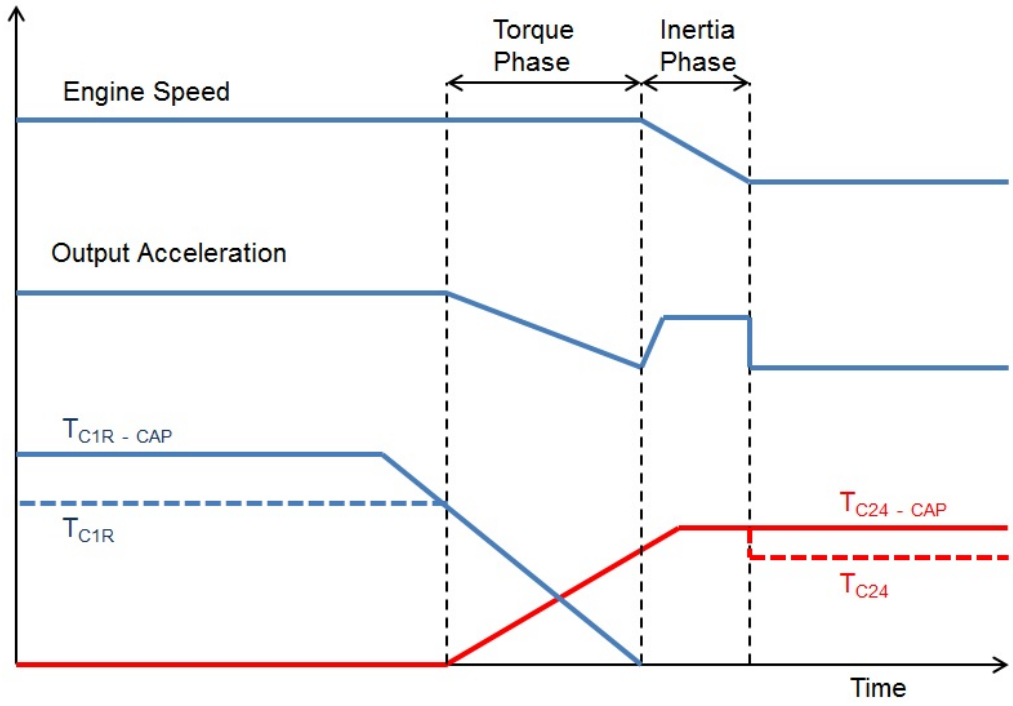

Figure 3.5: 1-2 Up-shift

where T_{out} is the output torque, I_{in} is the lumped inertia at the engine, and α is the acceleration or deceleration of the engine based on whether it is an down-shift or an up-shift.

For this example, since the speed at TISS will be reduced from the first gear level to the second gear level, α is negative. The clutch C24 will transmit the torque at full capacity until the desired engine speed is attained. This will cause the output torque to rise as shown in Fig. 3.5. Eventually, α goes to zero and the engine speed will reach the second gear level.

3.2.4 Down-shift

A similar approach is adopted for the down-shift control as shown in Fig. 3.6. But, the inertia phase occurs first as the gear ratio increases. The on-coming clutch (C1R) is filled and simultaneously, the engine speed is allowed to rise until it reaches the final desired

speed by releasing the pressure in the off-going clutch (C24). During this period, the rate of increase of the speed ratio is maintained at or above a specific value based on the requirement of shift duration. This can be done immediately after the shift command is given because it takes longer for the engine speed to rise than to complete the clutch fill. As the engine speed approaches the desired value, the torque phase begins and both the clutches are synchronized at calculated slopes similar to up-shift based on Eq. (3.6). The shift is completed when all the torque is transferred from clutch C24 to clutch C1R.

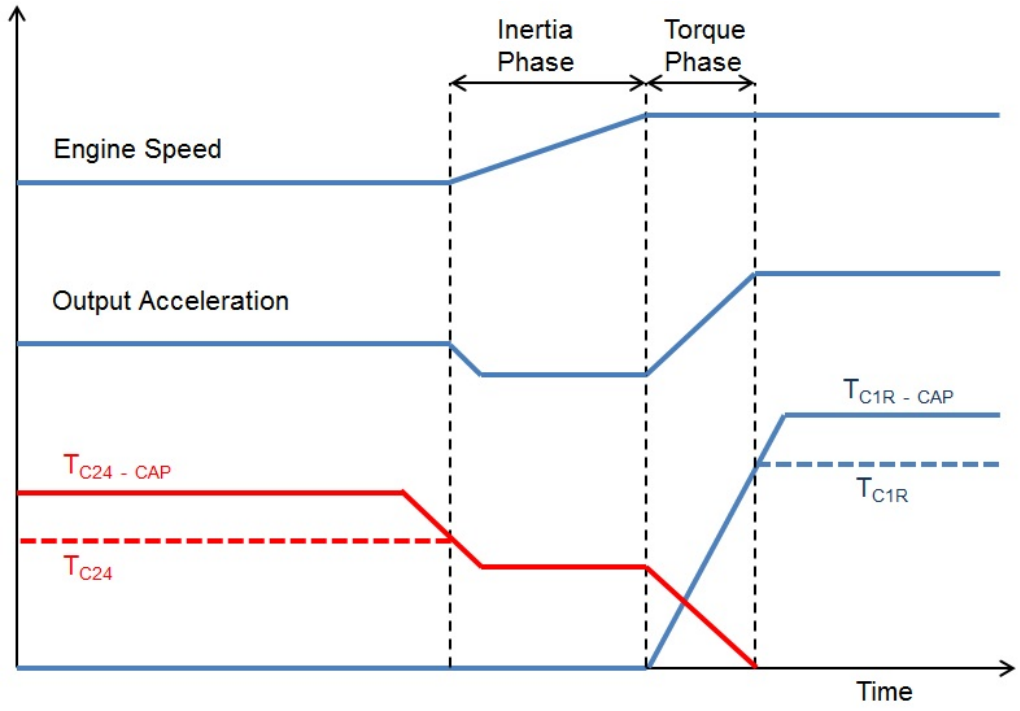

Figure 3.6: 2-1 Down-shift

Similarly, all the other shifts have been designed and controlled. The slopes of the pressure trajectories for the on-coming and off-going clutches are designed using Tab. 3.2 and their respective torque capacities.

Chapter 4

Hardware-in-the-loop Testing

Hardware-in-the-loop (HIL) is a common testing technique used in automotive industry to develop and validate real-time systems. It is very useful in scenarios where a component of a complicated system needs to be tested in the absence of the real system. Instead, the system is mathematically modeled and simulated, and is allowed to interact with the component in real-time with the help of sensors and actuators. This is an effective way to validate and measure its performance in real-time during its development phase. For this project, a HIL simulation is performed for the proposed transmission architecture to analyze its performance.

In this chapter, the experimental setup is discussed and the results are presented.

4.1 Experimental Setup

The setup for the hardware-in-the-loop (HIL) simulation is shown in Fig. 4.1. The entire powertrain is simulated in the computer and one of the clutches, C24, is replaced by a real clutch system. The choice of this clutch comes from the fact that C24 is involved in every gear shift after launch. Along with the hydraulics of remaining clutches (C1R, C123 and C34), the engine, torque converter, gearbox, and vehicle are all simulated using appropriate models. Clutch C1R is ignored in this implementation as it is used only for reverse gear. The clutch apparatus consists of the clutch piston, a pump, and a proportional pressure reducing valve. A ball valve is connected at the top to bleed the trapped air better instead of using the ball capsule. Unlike the real system, there

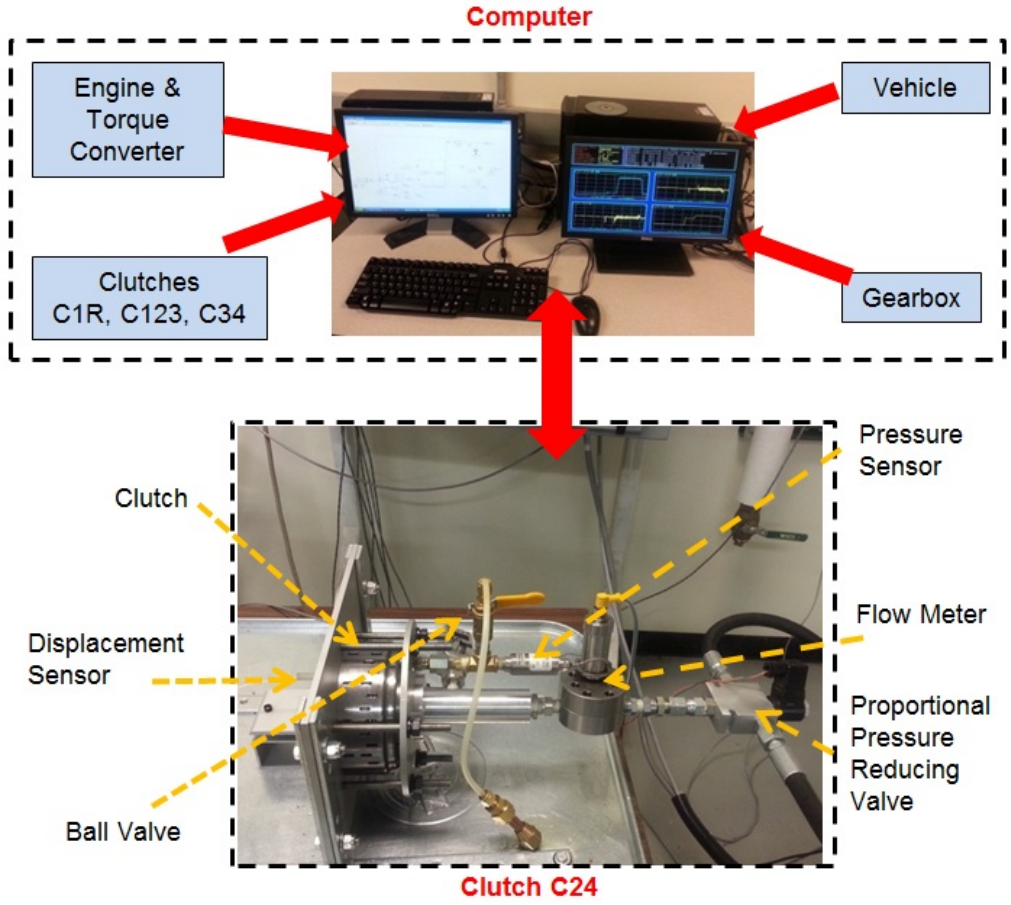

Figure 4.1: Setup for HIL Simulation

is no rotation of the clutch to evenly bleed the air through the ball capsules. This is very important to achieve good clutch fill due to the variation of bulk modulus at lower chamber pressures. The pressure sensor is also connected at the top of the chamber. The displacement sensor is a DVRT which is clamped in front of the clutch piston. The input voltage to control the proportional valve comes from the simulation, and the pressure and displacement measurements are sent back to the simulation. The pressure measurement is used as feedback to control the clutch and the displacement measurement is converted into torque capacity of the clutch to estimate its real torque capacity. Thus, the experiment progresses.

The hydraulics have been modeled using using the SimHydraulics package while the driveline model is created using MATLAB/Simulink functions in a host computer. The program uses two different sampling times which interact with each other during the experiment. The simulations are run at a time step of 0.1 ms, while the experiment runs at 1 ms. In simulations, larger time steps cause the simulation to fail at the hard stops and pressure chambers. This is due to the high stiffness of the system. Using smaller time step in experiments does not fetch better results as the time constants of the Proportional PRV and the clutch piston are relatively larger.

The model is then compiled to generate a C-code using a C-compiler. At the end of the build process, the C-code gets uploaded to the target computer which does all the computation required to implement the experiment. The SimHydraulics package in MATLAB is computationally intensive and the target computer does not possess high enough computing power. There are three main tasks that had to be completed before the model can be run successfully in real-time in the target computer. First, a more efficient C-compiler was identified and installed. This can be a critical issue when the time step is very close to the Task Execution Time (TET) value as in this case. The TET is the time taken by the computer to perform calculations for one time step. It should always be less than the time step. Initially, Watcom 1.9 C-compiler was used but it was found that the TET of the experiment with this compiler exceeded the time step of the model. So, Microsoft Visual Studio 10.0 was later used in this project which reduced the TET to $1/4^{\text{th}}$ of that of Watcom 1.9. Second, the solver settings and the convergence criterion for the model had to be relaxed. The consistency tolerance is set to $1e-5$ from the default $1e-9$ in the solver configuration block. Also, the fixed-cost run time consistency iterations is checked and the number of nonlinear iterations are reduced to 1. Third, the model was built with as few SimHydraulics blocks as possible and using m-functions wherever possible. Every block used from this package adds considerably to the computational burden.

Once this model is uploaded to the target computer, it is executed for an entire FTP driving cycle. The real clutch is characterized before beginning the cycle.

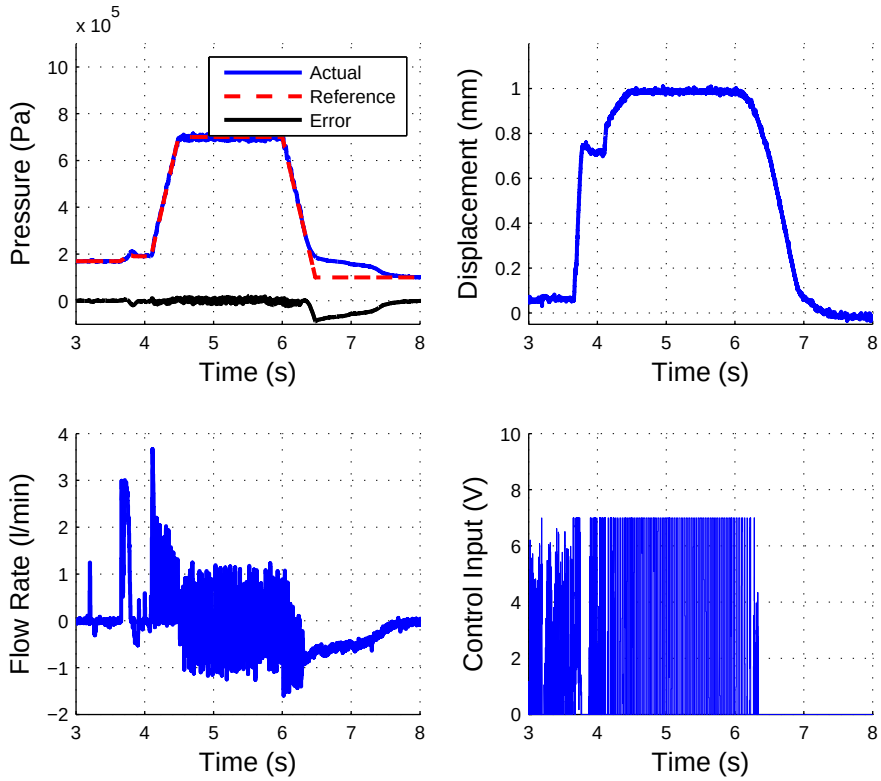

Figure 4.2: Clutch Characteristics

4.2 Clutch Characteristics

The real clutch system is shown in the Fig. 4.1. The clutch chamber is slightly pressurized to 1.6 bar in order to release the entrapped air. Due to static friction, the clutch piston does not move until the pressure reaches about 1.68 bar. It should travel 0.7 mm in about 0.25 s to successfully complete clutch fill. To achieve this, the pressure reference is increased from 1.68 bar to 1.97 bar in 0.15 s and then reduced to 1.91 bar in the next 0.05 s. Since the clutch piston comes in contact with the plates after the fill, the displacement between fill position and fully engaged position will be very small as it is due to the squeezing of the plates. During this period, the reference for the chamber pressure is linearly increased from 1.91 bar to 7 bar in 0.4 s to perform engagement.

The errors during clutch fill and engagement are well within acceptable range with the maximum error less than 0.2 bar. In case of aggressive air-bleeding, the piston may move before the clutch chamber is pressurized. The peak flow requirement of the clutch is 3.67 liter/min occurring at the beginning of the engagement when the proportional valve operates at full voltage. The maximum flow rate achievable through the smallest orifice in the hydraulic circuit is 4 liter/min for the given pressure settings.

The disengaging process follows a similar procedure. The pressure reference is linearly reduced from 7 bar to 1 bar in 0.48 s. The magnitude of error tends to increase at lower pressures as there is not enough flow to reduce the pressure as per the desired reference. The error grows large during this period but the clutch stops transmitting torque by then as the pressure is lower than the clutch fill pressure. The clutch characteristics along with the control input to the proportional valve are plotted in Fig. 4.2. The gains for the PID controller are documented in 4.1 for pressures measured in *psi*. As spool position of the proportional valve is also dependent on the clutch chamber pressure, the control input required to maintain the same spool position varies at different pressures. The controller outputs both positive and negative values while the proportional valve accepts only positive voltage inputs. So, a bias voltage is added to the controller input to restrict the controller output to 0 to 7 V using Eq. (2.23).

Table 4.1: PID controller gains

Clutch State	K_P	K_I	K_D
Steady (Low Pressure)	6	5.5	0.075
Fill	6	5.5	0.075
Engagement	8	7.5	0.25
Steady (High Pressure)	5	4.5	0.25
Disengagement	5	6	0.125

From Sec. 2.2.5, the clutch torque characteristics can be determined. It cannot be obtained directly from experiments as the clutch is a standalone apparatus in the laboratory and has no rotation or torque transmission. So, an indirect approach, using both

the clutch models and experiments, is employed to estimate the torque characteristics for this clutch. In this approach, the engagement force is calculated from the clutch model using its response from experiments as a function of the compression of the clutch plates.

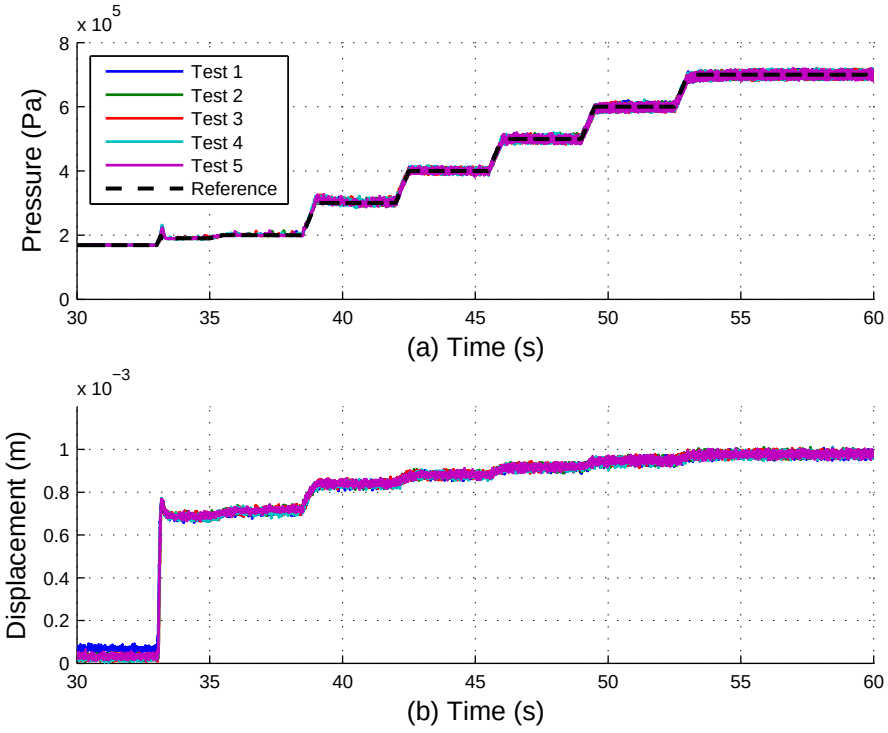

Figure 4.3: F_{eng} calibration: (a) Pressure (b) Displacement

The clutch chamber pressure tracked using a given reference and the resulting displacement are shown in Fig. 4.3. Figure 4.4 gives a better representation of the variation of the clutch displacement with its chamber pressure. The experiment is fairly repeatable and so, a reasonable map could be obtained. Using this data, the engagement force is estimated from the clutch model in Eq. (2.18). The mean of the pressure and displacement data from all the trials is converted to engagement force and plotted in Fig. 4.5. A 5th-order polynomial is fit through the data which is finally used for the experiments.

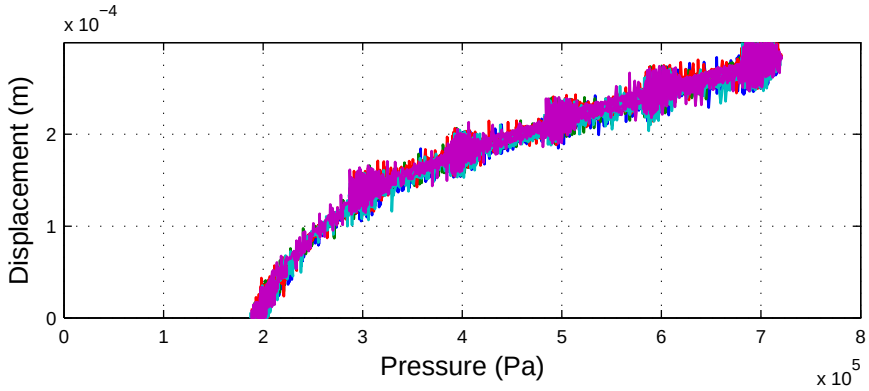

Figure 4.4: F_{eng} calibration: Pressure versus Displacement (after fill)

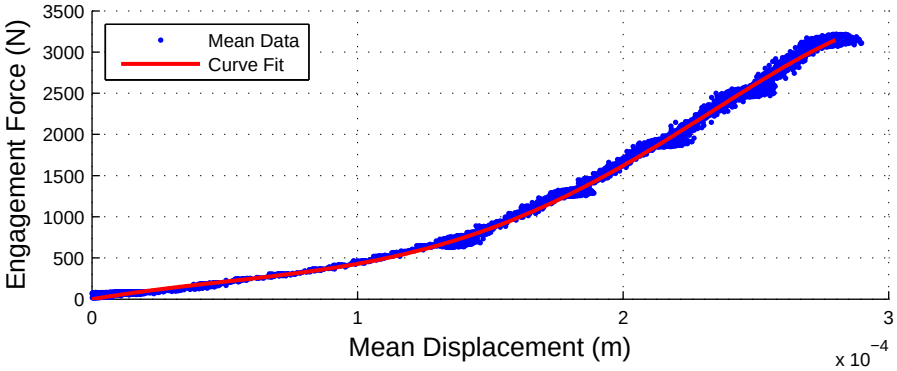

Figure 4.5: F_{eng} calibration: Engagement force versus Displacement (after fill)

4.3 FTP Cycle

4.3.1 Background

The United States Environmental Protection Agency, usually referred to as EPA, devised various driving cycles in order to test the emissions and fuel economies of vehicles under different conditions. Each testing cycle is called a Federal Test Procedure (FTP). FTP-75 and FTP-72 cycles are typically used to evaluate light-duty vehicles. FTP-75 cycle (See Fig. 4.6) is used to evaluate this new architecture. The entire FTP cycle consists of the following phases:

- Cold start transient phase (ambient temperature 20-30C), 0-505 s,
- Stabilized phase, $506 - 1372\,\mathrm{s}$,
- Hot soak (min 540 s, max 660 s),
- Hot start transient phase, $1372 - 1877\,\mathrm{s}$ (repeat of $0 - 505\,\mathrm{s}$).

Emissions from each phase are collected in a separate Teflon bag, analyzed and expressed in g/mile (g/km). The weighting factors are 0.43 for the cold start phase, 1.0 for the 'stabilized' phase and 0.57 for the hot start phase.

The following are some basic parameters of the cycle:.

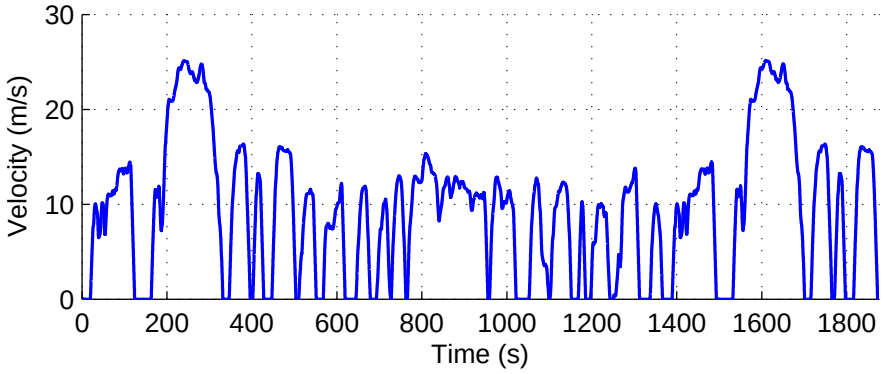

Figure 4.6: FTP Cycle: Vehicle Velocity

- Duration: 1877 s
- Distance traveled: 11.04 miles (17.77 km)
- Average speed: 21.2 mph (34.12 km/h).
- Maximum speed: 56.7 mph (91.25 km/h).

For emission certification, vehicles must meet the applicable FTP emission standards. From model year 2000, vehicles have to be additionally tested on two Supplemental Federal Test Procedures (SFTP) designed to address shortcomings with the FTP-75 in the representation of (1) aggressive, high speed driving (US06), and (2) the use of air conditioning (SC03). Fuel economy values are calculated on the basis of FTP testing for the city rating, while the highway rating is determined based on Highway Fuel Economy Testing (HWFET).

4.3.2 Implementation

Using the models and the control method described in the previous chapters, the complete EPA FTP-75 cycle has been performed to evaluate this new architecture. Even though this is a test for emissions, it can be used to test the reliability of this new architecture as the vehicle runs under a wide range of operating conditions during this cycle. To run this cycle, various input maps have to be generated such as the input engine torque, braking torque at the wheels, and the gear schedule map.

The FTP cycle is usually associated with the vehicle velocity profile (See Fig. 4.6). Using the velocity and acceleration, the tractive effort required to run the vehicle is computed from power-demand analysis. The braking torque is separately added as the engine cannot really provide negative torque assuming there is no engine braking. This tractive effort is then reflected back through the differential and the transmission to the torque converter output. And finally, the load is transferred to the engine using the torque converter model from Sec. 2.2.2. Based on the required engine speed and torque, the engine map is used to determine the throttle opening. The idling engine torque is set to 18.17 Nm and the angular speed to approximately 700 RPM. The throttle opening and the vehicle speed determine the occurrence of gear shifts with the help of the shift-scheduling chart from Fig. 3.1. These shifts are assumed to occur instantaneously

during these input map calculations. This procedure employed to obtain input maps is adapted from [47].

After the generation of these maps, the full FTP cycle test is performed in a HIL environment using the procedure described in earlier sections. The inputs to the simulation are the engine torque, braking torque at the wheels, and the gear schedule map as shown in Fig. 4.7. From the results shown in Fig. 4.8(a), it can be seen that the error in velocity is very small ($< 1\,\mathrm{m/s}$) even though it was assumed that the gear shifts occur instantaneously while generating input maps. The vehicle acceleration for the entire cycle can be seen in Fig. 4.8(b). In Fig. 4.8(c) and (d), the speed and torque of the engine and the turbine side of the torque converter are plotted. An amplification of torque can be observed at the torque converter with speed reduction. Also, with the engine speed reaching only a maximum of 2800 RPM, the FTP cycle can be said to be fairly conservative.

To clearly study the quality of the shifts with this new architecture, a few shifts have been chosen to demonstrate the performance during this entire cycle. They have been marked in red in Fig. 4.7(c). It is desirable that the entire gear shift be completed within 1 s and the duration of the shift the user experiences be limited to 0.5 s, which is the summation of the time taken to complete torque and inertia phases. The plots are made between the chamber pressures of the on-coming and off-going clutches. Simultaneously, the torque capacities and the torques carried by these clutches are plotted. The oscillations in the pressure and torque capacity are due to the dynamics of the clutch piston. The high stiffness of the clutch plates and to some extent, the pressure control as well, contribute to these oscillations of clutch piston. Even a minor error in tracking pressure can affect the displacement. To analyze the impact of the shifts on the vehicle performance, the vehicle acceleration is plotted. The speed ratio is also shown, which is the ratio between the turbine speed of the torque converter and the output of the transmission. The engine and turbine speeds are plotted to study the effect on the engine side.

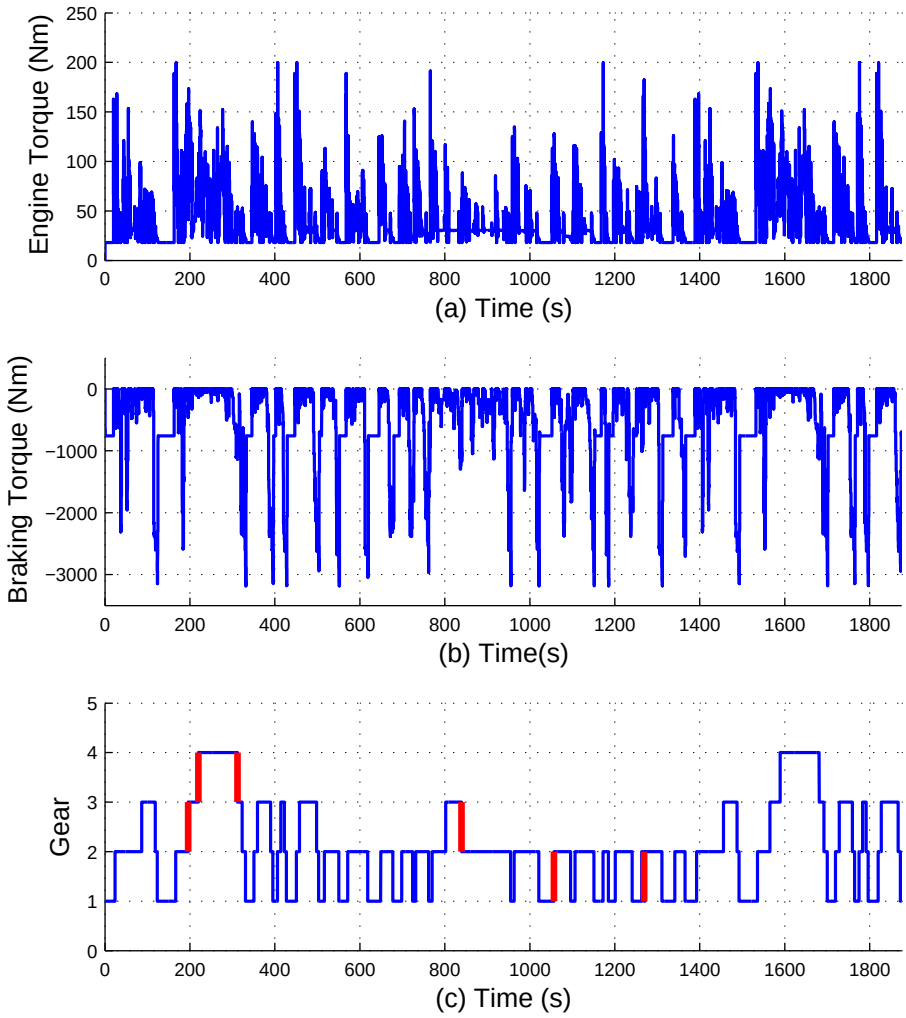

Figure 4.7: FTP Cycle: Input Maps (a) Engine torque (b) Braking Torque at the wheels (c) Gear Schedule

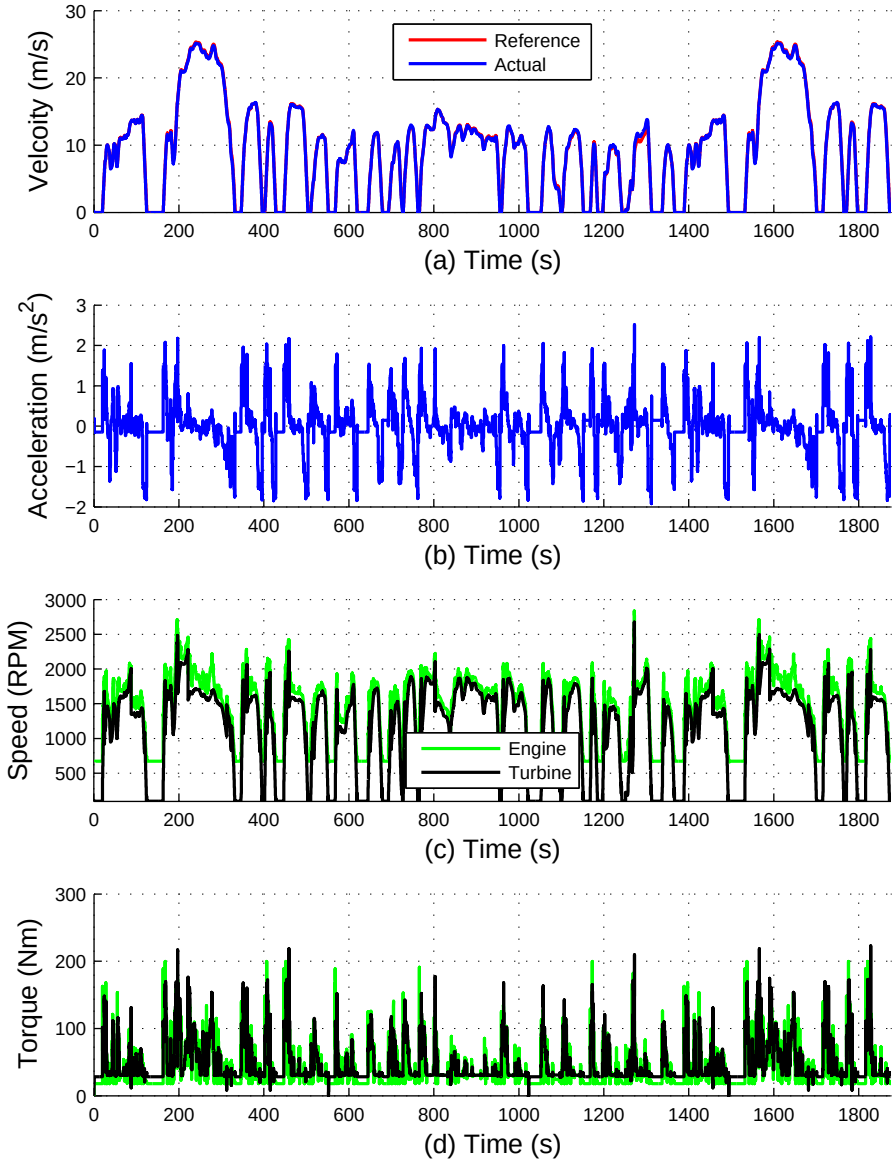

Figure 4.8: FTP Cycle: Results (a) Vehicle Velocity (b) Vehicle Acceleration (c) Engine and Turbine speeds

4.3.3 1-2 Up-shift

The 1-2 up-shift occurs very frequently in this cycle as the vehicle is brought to rest and restarted many number of times. Figure 4.9 is an up-shift occurring as clutch C1R synchronizes with the clutch C24. The effect of overfill of clutch C24 can be seen with the torque capacity rising prematurely. The off-going clutch C1R is released until a blip in the speed ratio is observed and immediately the clutches are synchronized. As the torque gets transferred to the clutch C24, the oscillations in the acceleration can be observed from the piston dynamics. The oscillations do not affect the engine speed due to the torque converter. The entire shift duration is 0.94 s and the torque and inertia phases take place in 0.23 s.

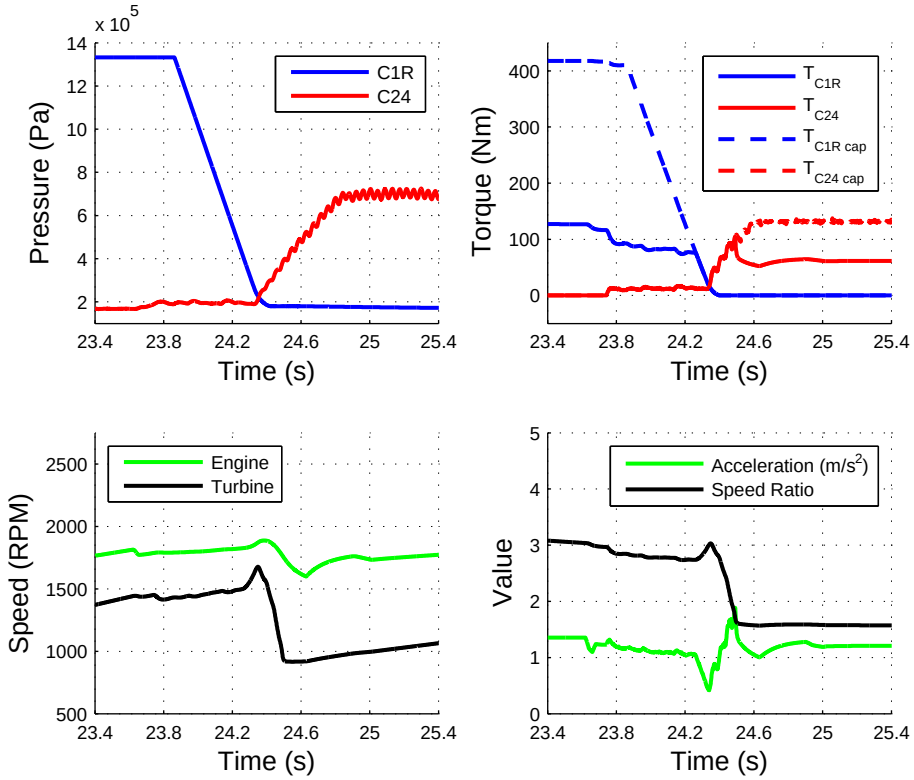

Figure 4.9: 1-2 Up-shift

4.3.4 2-3 Up-shift

In the 2-3 up-shift, the off-going clutch is C24 and the on-coming clutch is C34. As the torque carried by the clutches is lower during this period, the off-going clutch C24 disengages almost completely to observe a slight increase in speed ratio before the on-coming clutch C34 is engaged. Due to the nature of the algorithm, the C34 is directly connected to the pump once the capacity of C24 reduces to zero. This causes its torque capacity to rise very steeply and is seen in the acceleration as a spike. It brings the engine speed to the new level very quickly as shown in Fig. 4.10. This is due to the absence of inertia phase control during up-shifts. The user experiences 0.141 s out of the total 0.844 s long shift.

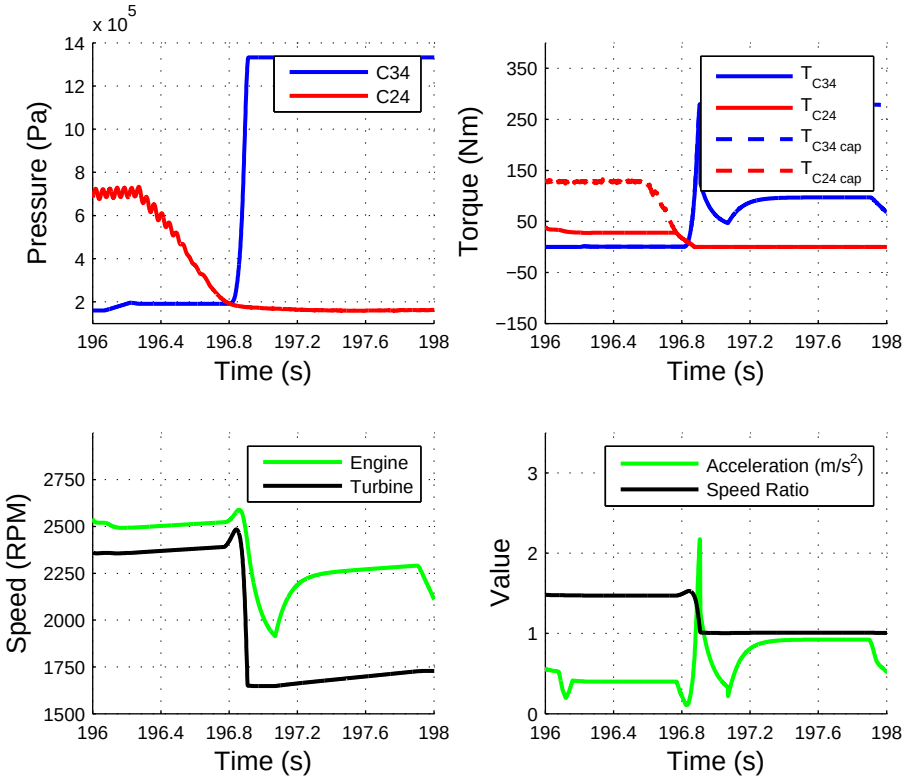

Figure 4.10: 2-3 Up-shift

4.3.5 3-4 Up-shift

The 3-4 up-shift is very similar to the 2-3 up-shift in terms of its behavior as seen in Fig. 4.11. The torque supplied by the engine is lower and therefore, it takes much longer to cause the speed ratio to change. Again, it results in the off-going clutch C123 being almost fully disengaged before the on-coming clutch C24 is engaged. The torque directions are opposite but that it does not affect the reference slopes. The torque and inertia phases last for 0.145 s while the entire shift lasts for 1.55 s. A more aggressive shifting strategy can be designed when the torque carried is low.

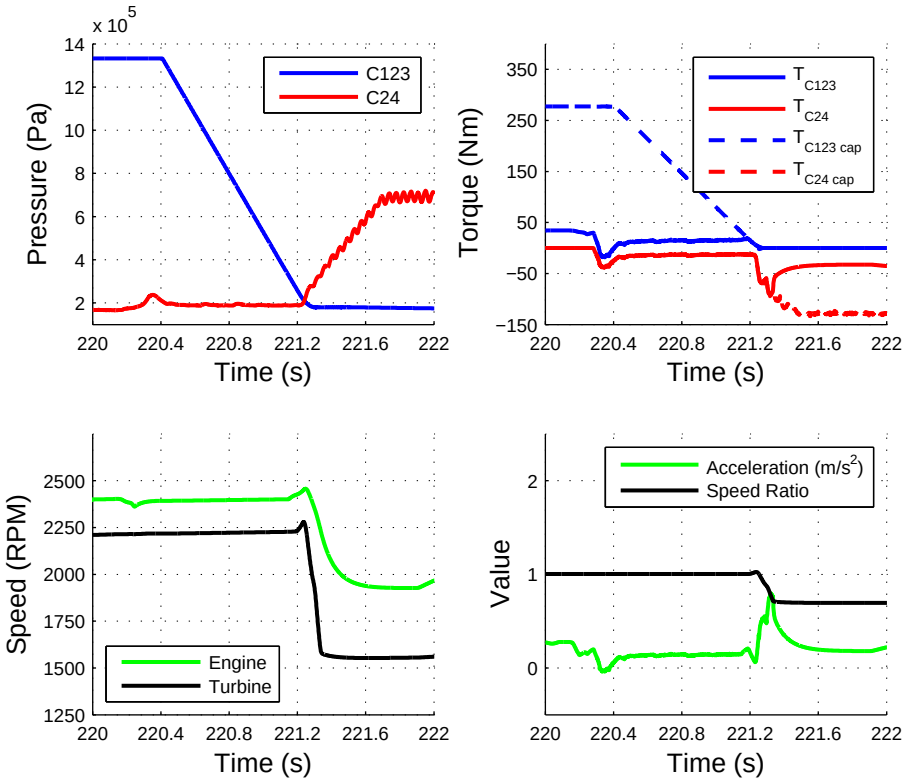

Figure 4.11: 3-4 Up-shift

4.3.6 2-1 Down-shift

The 2-1 down-shift occurred mostly before coming to rest except in a couple of cases where the speed was reduced. During the inertia phase, the speed ratio increases to the desired value through controlled disengagement of the off-going clutch C24. At the end of this phase, the remaining torque of the clutch C24 is synchronized with clutch C1R. This shift takes place relatively faster as the engine torque is higher which will accelerate the engine at a quicker rate. The duration of this shift is approximately 0.725 s and the inertia and torque phases last 0.229 s.

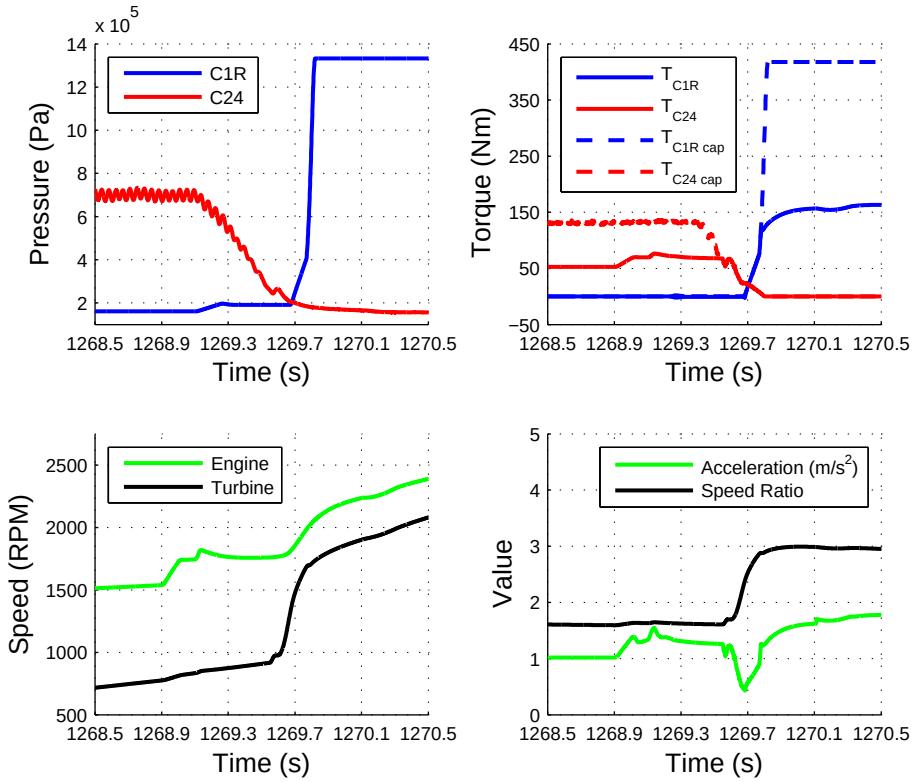

Figure 4.12: 2-1 Down-shift

4.3.7 3-2 Down-shift

The algorithm is the same for the 3-2 down-shift but the rate of speed ratio increase is different for each shift during inertia phase. Even though the torque in clutch C34 is low, it is increased due to an overfill from clutch C24 as they are counteracting torques. This is particularly useful because the speed ratio increases at a faster rate and the torques are easier to synchronize with larger magnitudes. It can be used as a strategy to rise the engine speed at low torques during down-shifts. It should be noted that it can cause the vehicle to accelerate which is undesirable during braking. It takes 1.15 s to complete the shift while it requires 0.25 s to initiate and complete the inertia and torque phases.

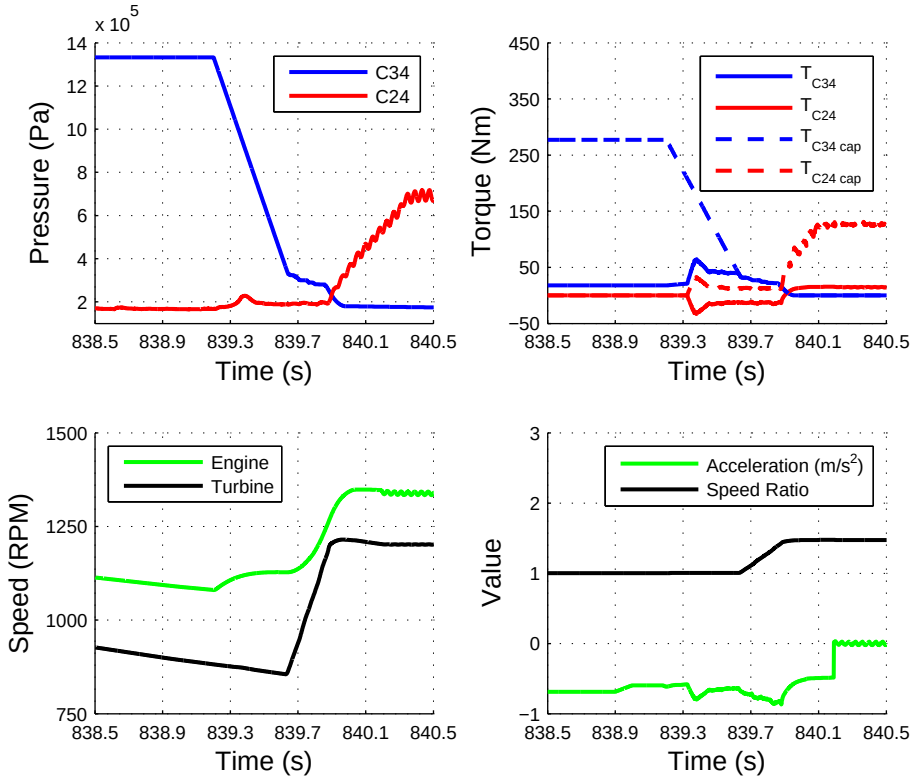

Figure 4.13: 3-2 Down-shift

4.3.8 4-3 Down-shift

The 4-3 down-shift occurs only twice in the entire cycle. In both the cases, the vehicle experiences sudden braking and comes to rest in a short span of time. Due to the small torque carried by off-going clutch C24, it can be inferred that the engine torque is small. So, even after reducing its torque capacity to zero, the engine does not flare. It can be achieved faster if the on-coming clutch C123 is engaged earlier. But, unlike 3-2 down-shift, there is no overfill here to enhance the rate. So, the shift period is 0.847 s and the inertia and torque phase periods together is 0.244 s.

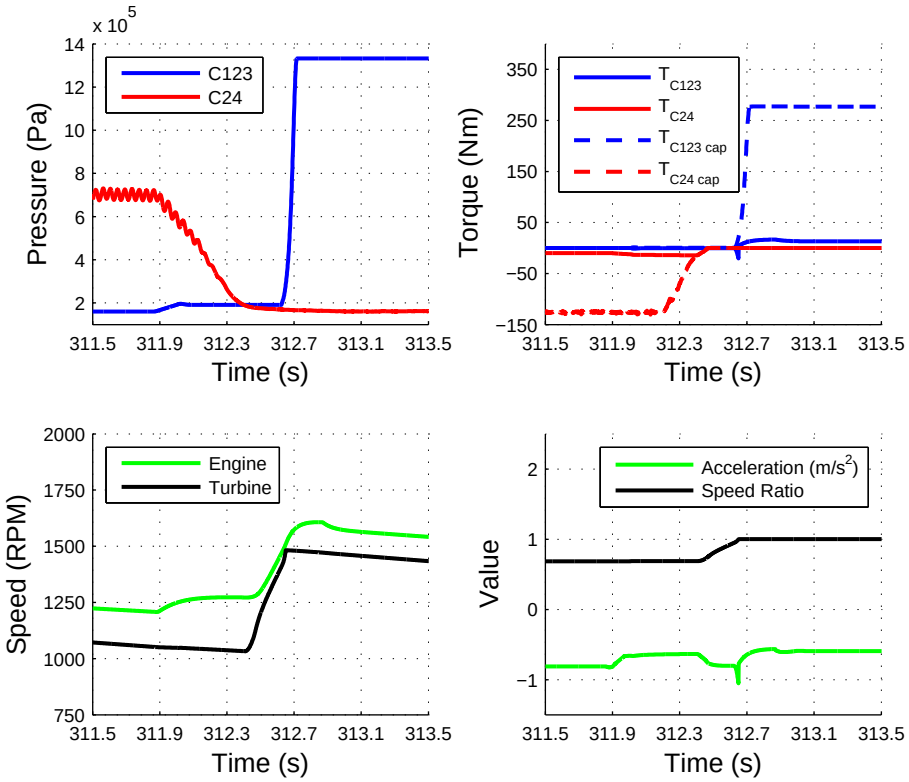

Figure 4.14: 4-3 Down-shift

4.3.9 Summary

From the FTP cycle, a few shifts have been chosen to study and evaluate the performance of the architecture. The shifts mostly conform to the criteria specified except at lower torques. Most of the shifts complete within 1 s with inertia and torque phases lasting well below 0.5 s. There are a few overfills that occur with the on-coming clutch but the control algorithm is quite robust to it. The accelerations during down-shifts are very well regulated by controlling the inertia phase. But, the inertia phase has not been controlled during up-shifts which caused occasional peaks in acceleration. Also, at lower input torques, the engine speed rises very slowly as seen in 3-4 up-shift and 3-2 down-shift. A more aggressive disengaging strategy can handle this issue provided this condition can be identified. Overfills or early engagement could help accelerate the shift in these conditions but it will accelerate the vehicle too which is undesirable under braking. Overall, the architecture meets the preliminary targets to a satisfactory level.

Chapter 5

Summary and Conclusion

A new architecture has been proposed for the automatic transmission system. The architecture requires that the clutches contain pressure sensors as the feedback elements. It simplifies the transmission hydraulic system and makes it more flexible for adapting it to transmissions with greater number of speeds. The feedback element reduces the calibration effort required as the clutches can now be controlled in closed-loop using pressure feedback. In order to test this architecture, all the driveline elements have been simulated using models from literature. Since the steady state performance of this architecture will be similar to the current architecture, it has been evaluated through gear shifts. The gear shifting strategy for the current system is adapted for this new architecture. The control algorithm uses the pressure feedback from the clutches in addition to the feedback from the input and output speed sensors of transmission. The clutch chamber pressure has been found to have a direct correlation to the torque capacity of a clutch during engagement and disengagement. This was useful to implement a closed loop control during gear shifts.

The architecture was then validated by conducting experiments in a HIL environment using the driveline model and a real clutch setup. The engagement force of the real clutch has been characterized using experiments and models. The performance of the architecture for an entire EPA FTP driving cycle is presented as it provides a variety of operating conditions to test this architecture. To analyze the gear shift quality, a few shifts are chosen for detailed analysis. The simulated clutches were synchronized with the real clutch during gear shifts. The results show that the performance of the

proposed architecture is able to meet the preliminary targets.

Future work could include developing more aggressive gear shifting strategies as the feedback gives greater control of the clutches. Another possible extension would be to design optimal shift trajectories based on required flow rate for the clutch chamber pressures. High pressure control could be developed to downsize the pump further and make the system more compact.

References

[1] G. Wagner. Application of transmission systems for different driveline configurations in passenger cars. *SAE Technical Paper*, (2001–01–0882), 2001.

[2] G. Genta and L. Morello. *The Automotive Chassis: Vol. 1: Components Design*. Springer, 2009.

[3] L. Glielmo, L. Iannelli, V. Vacca, and F. Vasca. Gearshift control for automated manual transmissions. *IEEE/ASME Transactions on Mechatronics*, 11(1):17–26, 2006.

[4] X. Song, Z. Sun, X. Yang, and G. Zhu. Modelling, control, and hardware-in-the-loop simulation of an automated manual transmission. *Proceedings of the Institution of Mechanical Engineers, Part D: Journal of Automobile Engineering*, 224(2):143–160, 2010.

[5] Y. Zhang, X. Chen, X. Zhang, H. Jiang, and W. Tobler. Dynamic modeling and simulation of a dual-clutch automated lay-shaft transmission. *Transactions of the ASME-R-Journal of Mechanical Design*, 127(2):302–307, 2005.

[6] M. Kulkarni, T. Shim, and Y. Zhang. Shift dynamics and control of dual-clutch transmissions. *Mechanism and Machine Theory*, 42(2):168–182, 2007.

[7] B. Matthes. Dual clutch transmissions - lessons learned and future potential. *SAE Technical Paper*, (2005–01–1021), 2005.

[8] T. Grewe, B. Conlon, and A. Holmes. Defining the general motors 2-mode hybrid transmission. *SAE Technical Paper*, (2007–01–0273), 2007.

[9] S. Kim, J. Park, J. Hong, M. Lee, and H. Sim. Transient control strategy of hybrid electric vehicle during mode change. *SAE Technical Paper*, (2009–01–0228), 2009.

[10] N.J. Schouten, M.A. Salman, and N.A Kheir. Fuzzy logic control for parallel hybrid vehicles. *IEEE Transactions on Control Systems Technology*, 10(3):460–468, 2002.

[11] P. Setlur, J.R. Wagner, D.M. Dawson, and B. Samuels. Nonlinear control of a continuously variable transmission (cvt). *Control Systems Technology, IEEE Transactions on*, 11(1):101–108, 2003.

[12] N. Srivastava and I. Haque. A review on belt and chain continuously variable transmissions (cvt): Dynamics and control. *Mechanism and machine theory*, 44(1):19–41, 2009.

[13] Z. Sun and K. Hebbale. Challenges and opportunities in automotive transmission control. In *American Control Conference, 2005. Proceedings of the 2005*, pages 3284–3289. IEEE, 2005.

[14] F. Vasca, L. Iannelli, A. Senatore, and G. Reale. Torque transmissibility assessment for automotive dry-clutch engagement. *IEEE/ASME Transactions on Mechatronics*, 16(3):564–573, 2011.

[15] E.J. Berger, F. Sadeghi, and C.M. Krousgrill. Torque transmission characteristics of automatic transmission wet clutches: Experimental results and numerical comparison. *Tribology Transactions*, 40(4):539–548, January 1997.

[16] D.A. Crolla. *Automotive engineering: powertrain, chassis system and vehicle body*. Butterworth-Heinemann, 2009.

[17] H.C. Miao, Z. Sun, J. Fair, J. Lehrmann, and S. Harbin. Modeling and analysis of the hydraulic system for oil budget in an automotive transmission. *ASME DSCD Conference Proceedings*, pages 455–462, 2008.

[18] S. Watechagit and K. Srinivasan. Modeling and simulation of a shift hydraulic system for a stepped automatic transmission. *SAE Technical Paper*, (2003–01–0314), 2003.

[19] G. Tao, T. Zhang, and H. Chen. Modeling of shift hydraulic system for automatic transmission. In *Consumer Electronics, Communications and Networks (CECNet), 2011 International Conference on*, pages 474–477. IEEE, 2011.

[20] B. Cho, J. Oh, and W. Lee. Modeling of pulse width modulation pressure control system for automatic transmission. *SAE Technical Paper*, (2002–01–1257), 2002.

[21] H. Tsutsui, T. Hisano, A. Suzuki, M. Hijikata, M. Taguchi, and K. Kojima. Electro-hydraulic control system for aisin aw new 6-speed automatic transmission. *SAE Technical Paper*, (2004–01–1638), 2004.

[22] W. Shuhan, X. Xiangyang, L. Yanfang, and D. Zhenkun. Dynamic characteristic simulation of at hydraulic system. *SAE Technical Paper*, (2008–01–1683), 2008.

[23] T. Ohashi, S. Asatsuke, H. Moriya, and T.R. Noble. Honda's 4 speed all clutch to clutch automatic transmission. *SAE Technical Paper*, (980819), 1998.

[24] H. Wakamatsu, T. Ohashi, S. Asatsuke, and Y. Saitou. Honda's 5 speed all clutch to clutch automatic transmission. *SAE Technical Paper*, (2002–01–0932), 2002.

[25] D. Kusamoto, Y. Yasuda, K. Watanabe, H. Kimura, and A. Hoshino. Toyota's new six-speed automatic transaxle u660e for fwd vehicles. *SAE Technical Paper*, (2006–01–0847), 2006.

[26] H. Ota, K. Nozaki, A. Honda, M. Kinoshita, et al. Toyota's world first 8-speed automatic transmission for passenger cars. *SAE Technical Paper*, (2007–01–1101), 2007.

[27] S. Bai, R.L. Moses, T. Schanz, and MJ Gorman. Development of a new clutch-to-clutch shift control technology. *SAE Technical Paper*, (2002–01–1252), 2002.

[28] T. Minowa, T. Ochi, Kuroiwa H., and K. Liu. Smooth gear shift control technology for clutch-to-clutch shifting. *SAE Technical Paper*, (1999–01–1054), 1999.

[29] S. Wentao and C. Huiyan. Research on control strategy of shifting progress. *SAE Technical Paper*, (2008–01–1684), 2008.

[30] R. Dixon. Outlook for safety and powertrain sensors. *Advanced Microsystems for Automotive Applications 2012*, pages 343–352, 2012.

[31] X. Song and Z. Sun. Pressure-based clutch control for automotive transmissions using a sliding-mode controller. *IEEE/ASME Transactions on Mechatronics*, 17(3):534–546, 2012.

[32] K. Hagiwara, S. Terayama, Y. Takeda, K. Yoda, and S. Suzuki. Development of automatic transmission control system using hardware-in-the-loop simulation system. *JSAE Review*, 23(1):55–59, January 2002.

[33] F.V. BrandAao, D.F Kelly, and K. Fan. Using model, software and hardware-in-loop to develop automated transmission. *SAE Technical Paper*, (2007–01–2581), 2007.

[34] L. Mianzo. A transmission model for hardware-in-the-loop powertrain control system software development. In *Control Applications, 2000. Proceedings of the 2000 IEEE International Conference on*, pages 1–8. IEEE, 2000.

[35] Q. Zheng, W. Chung, K. Defore, and A. Herman. A hardware-in-the-loop test bench for production transmission controls software quality validation. *SAE Technical Paper*, (2007–01–0502), 2007.

[36] M.S. Castiglione, G. Stecklein, R. Senseney, and D. Stark. Development of transmission hardware-in-the-loop test system. *SAE Technical Paper*, (2003–01–1027), 2003.

[37] Q. Zheng, J. Kraenzlein, E. Hopkins, R.L. Moses, and B. Olson. Closed loop pressure control system development for an automatic transmission. *SAE Technical Paper*, (2009–01–0951), 2009.

[38] D. Cho and J.K. Hedrick. Automotive powertrain modeling for control. *Journal of Dynamic Systems, Measurement, and Control*, 111(4):568–576, 1989.

[39] A.J. Kotwicki. Dynamic models for torque converter equipped vehicles. *SAE Technical Paper*, (820393), 1982.

[40] A. Crowther, N. Zhang, D.K. Liu, and J.K. Jeyakumaran. Analysis and simulation of clutch engagement judder and stick-slip in automotive powertrain systems. *Proceedings of the Institution of Mechanical Engineers, Part D: Journal of Automobile Engineering*, 218(12):1427–1446, 2004.

[41] S. Watechagit. *Modelling and Simulation of a Shift Hydraulic System for a Stepped Automatic Transmission*. PhD thesis, Ohio State University, 2003.

[42] P. Samanuhut and A. Dogan. Dynamics equations of planetary gear sets for shift quality by lagrange method. *ASME DSCD Conference Proceedings*, pages 353–360, 2008.

[43] C.E. Burke, L. Nagler, E. Campbell, L. Lundstrom, et al. Where does all the power go? *SAE Technical Paper*, (570058), 1957.

[44] P.N. Blumberg. Powertrain simulation: A tool for the design and evaluation of engine control strategies in vehicles. *SAE Technical Paper*, (760158), 1976.

[45] R.L. Bechtold. Ingredients of fuel economy. *SAE Technical Paper*, (790928), 1979.

[46] H.L. Benford and M.B. Leising. The lever analogy: A new tool in transmission analysis. *SAE Technical Paper*, (810102), 1981.

[47] A. Heinzen, P. Gillella, and Z. Sun. Iterative learning control of a fully flexible valve actuation system for non-throttled engine load control. *Control Engineering Practice*, 19(12):1490–1505, December 2011.

Appendix A

Simulink Models

A.1 Real-Time Model

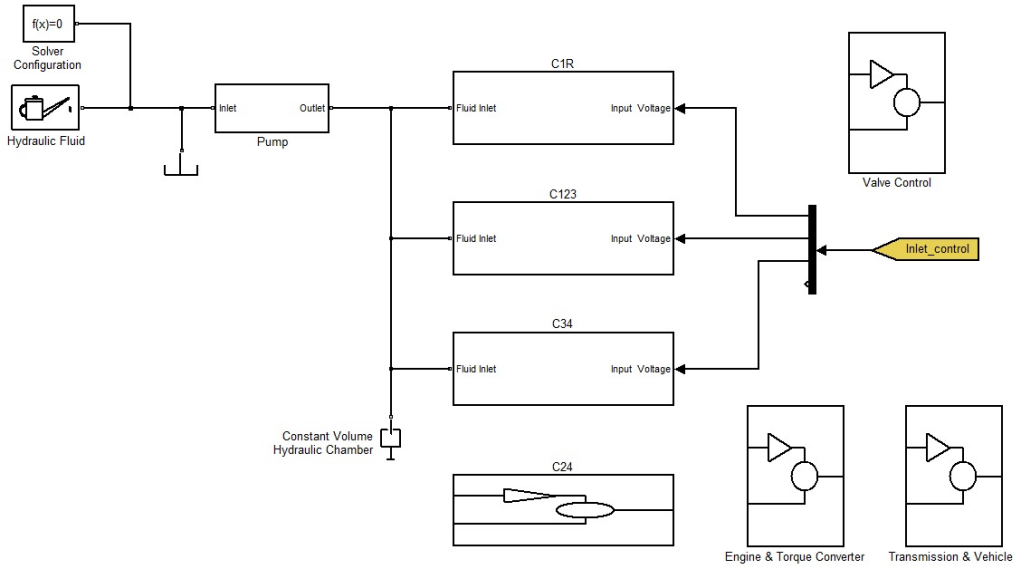

Figure A.1: High level real-time model

A.2 Driveline Elements

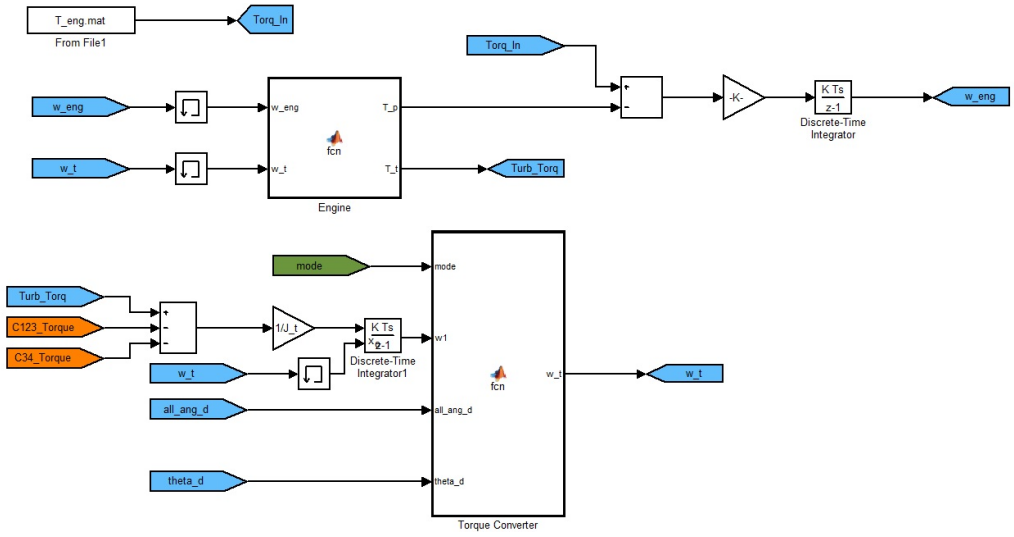

Figure A.2: Engine and Torque Converter

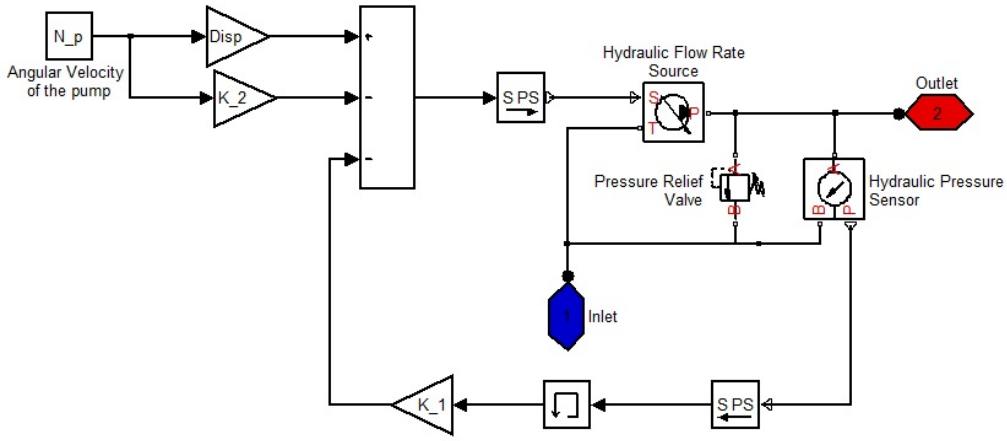

Figure A.3: Pump model

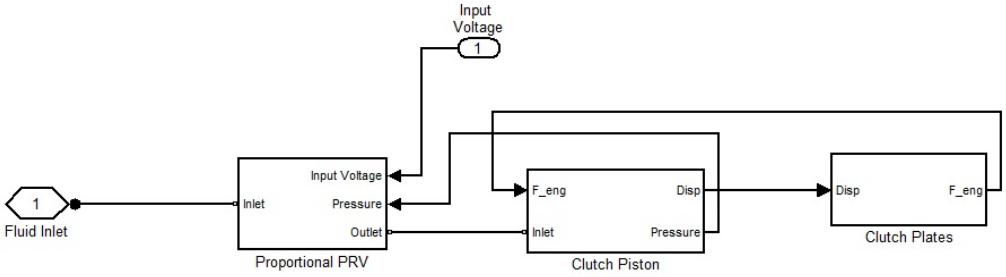

Figure A.4: Simulated clutch system

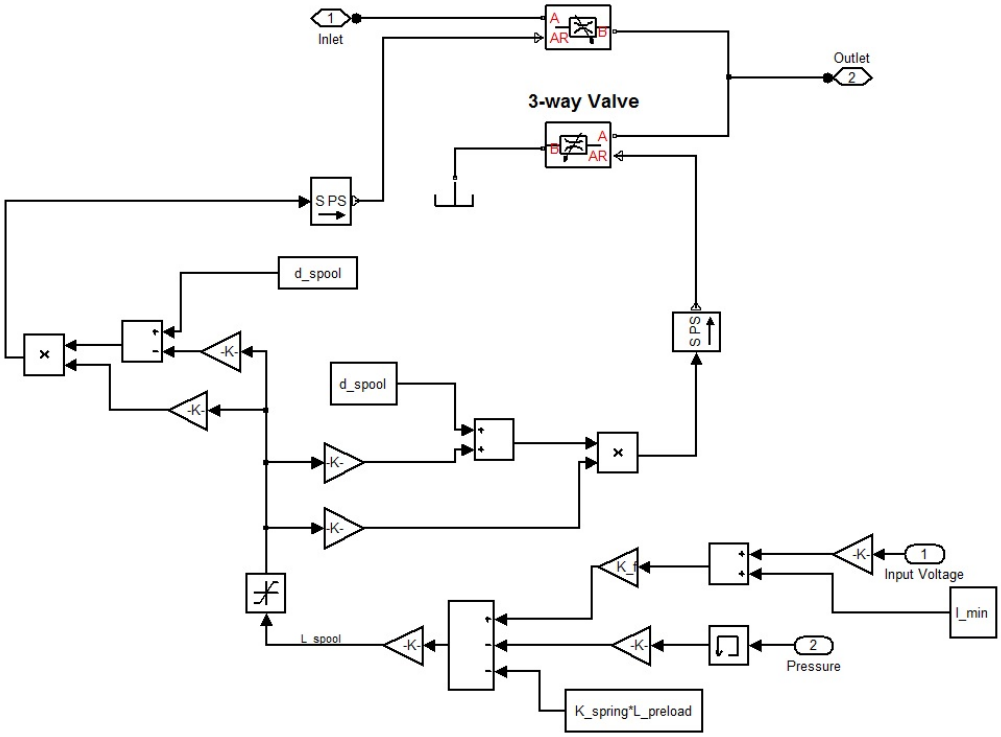

Figure A.5: Proportional PRV model

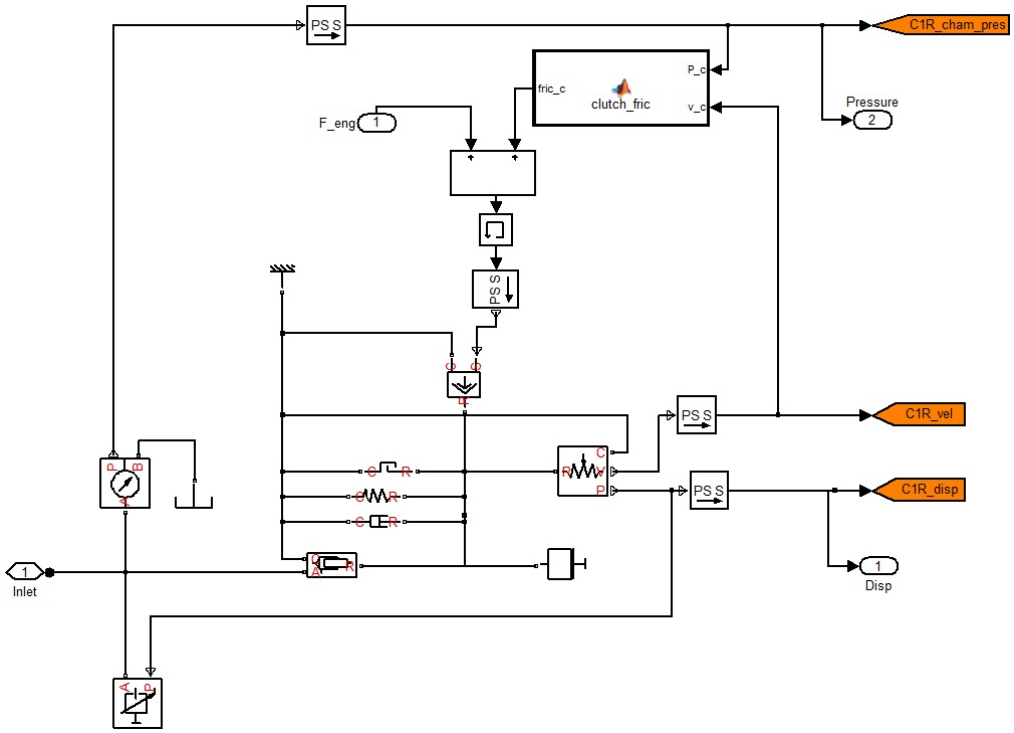

Figure A.6: Simulated clutch piston model

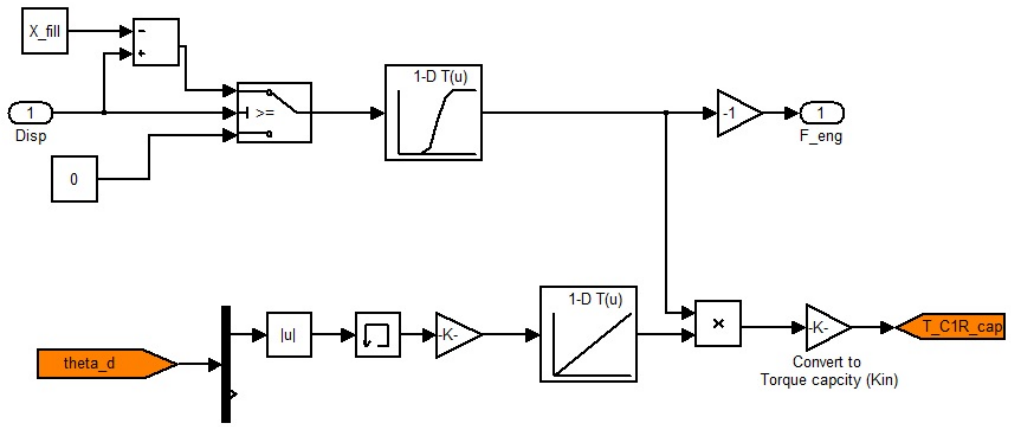

Figure A.7: Engagement force model

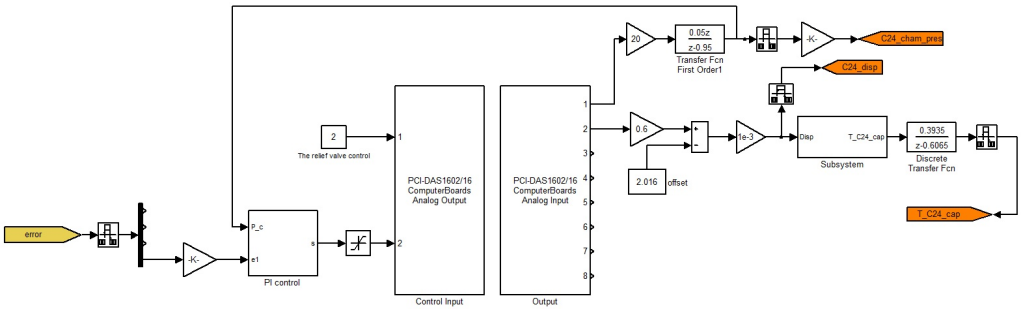

Figure A.8: Real clutch system

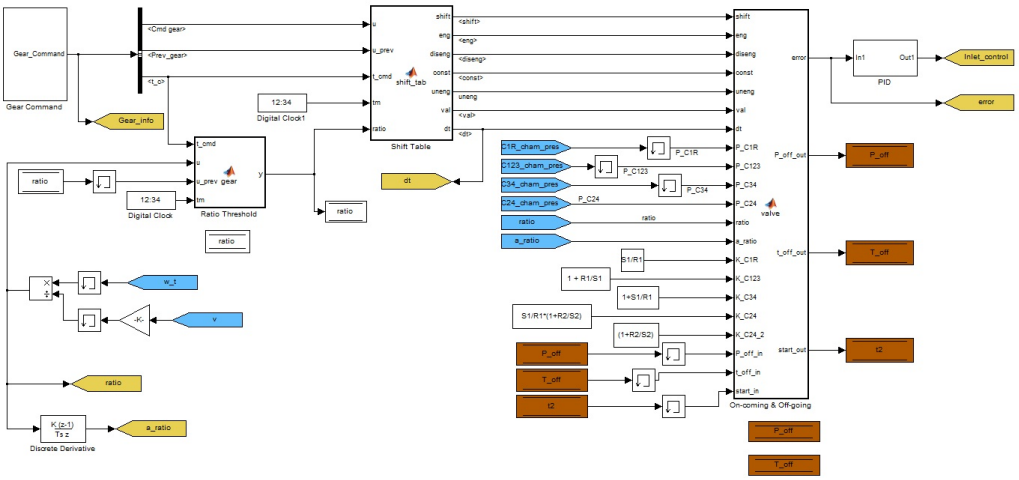

Figure A.9: Valve Control

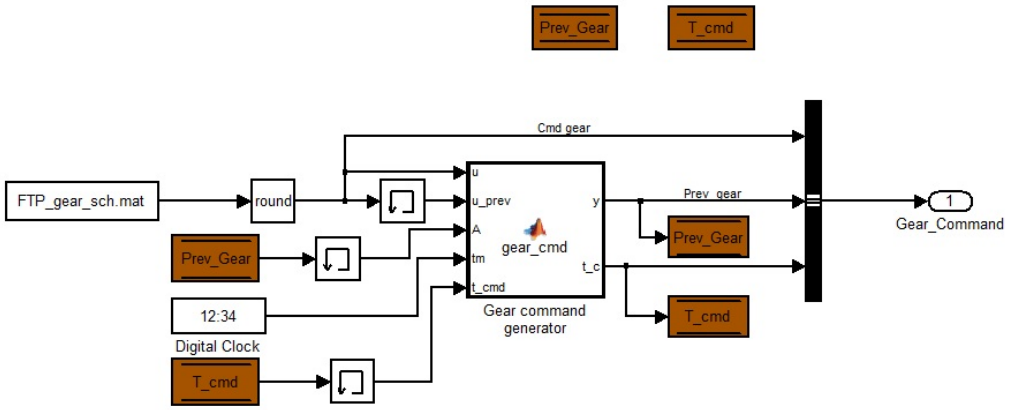

Figure A.10: Command gear generator

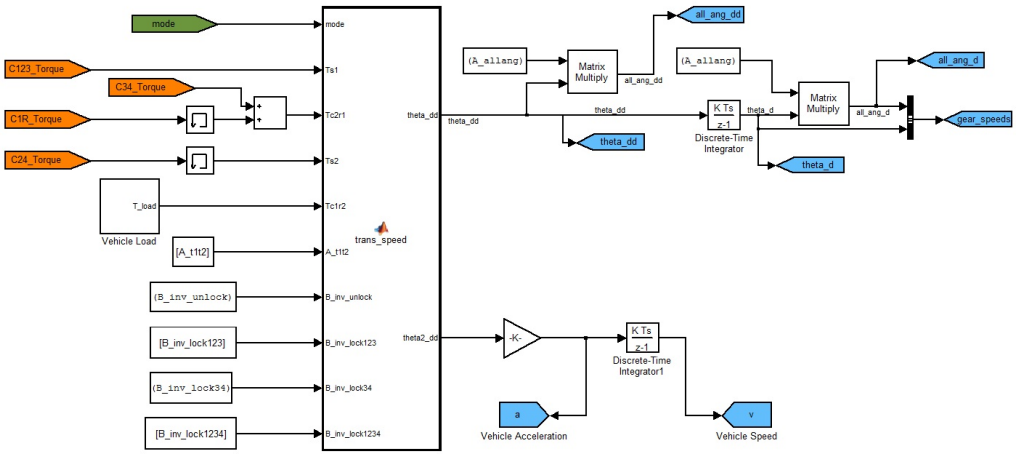

Figure A.11: Planetary gear set model

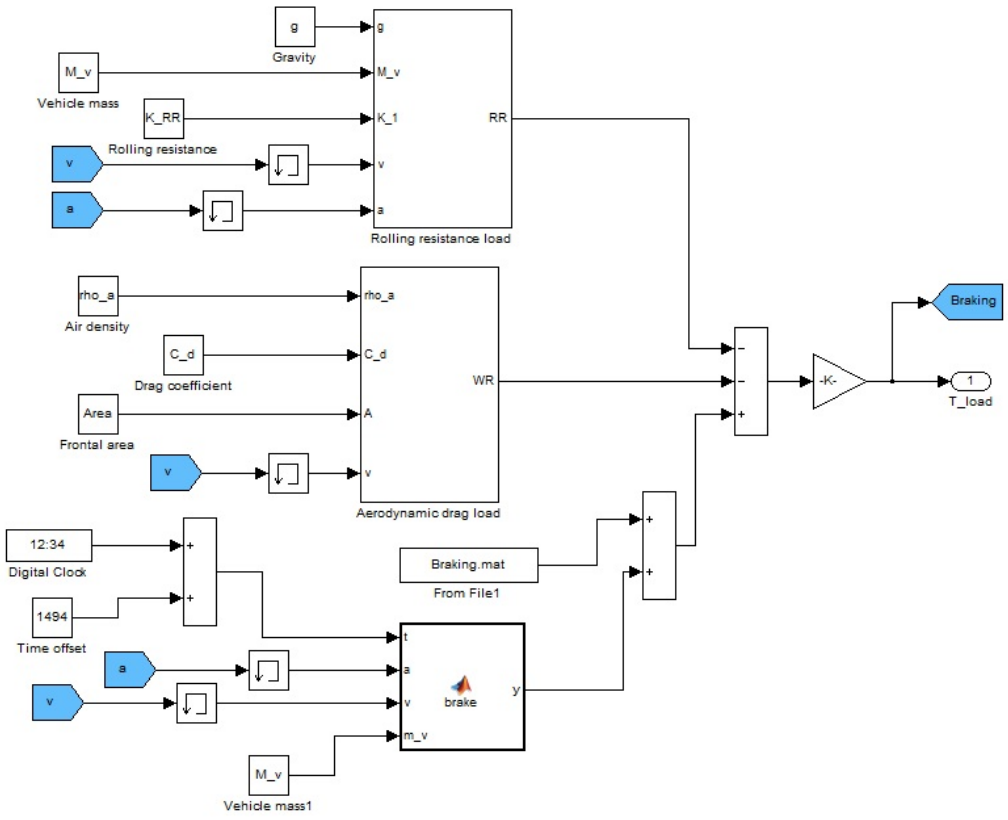

Figure A.12: Vehicle load model